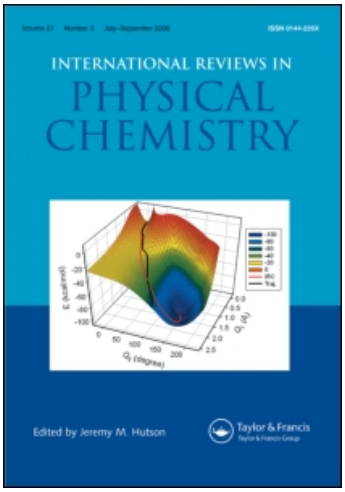

International Reviews in Physical Chemistry
Publication details, including instructions for authors and subscription information:
http://www.informaworld.com/smpp/title~content=t713724383

Spectroscopy of free radicals and radical containing entrance-channel complexes in superfluid helium nanodroplets

Jochen Küpper[ab]; Jeremy M. Merritt[ab]
[a] Fritz-Haber-Institut der MPG, 14195 Berlin, Germany [b] University of North Carolina, Chapel Hill, NC 27599, USA

To cite this Article Küpper, Jochen and Merritt, Jeremy M.(2007) 'Spectroscopy of free radicals and radical containing entrance-channel complexes in superfluid helium nanodroplets', International Reviews in Physical Chemistry, 26: 2, 249 — 287
To link to this Article: DOI: 10.1080/01442350601087664
URL: http://dx.doi.org/10.1080/01442350601087664

International Reviews in Physical Chemistry,
Vol. 26, No. 2, April–June 2007, 249–287

Taylor & Francis
Taylor & Francis Group

Spectroscopy of free radicals and radical containing entrance-channel complexes in superfluid helium nanodroplets

JOCHEN KÜPPER* and JEREMY M. MERRITT†

Fritz-Haber-Institut der MPG, Faradayweg 4–6, 14195 Berlin, Germany,
and University of North Carolina, Chapel Hill, NC 27599, USA

Dedicated to Roger E. Miller

(*Received 6 September 2006; in final form 26 October 2006*)

The spectroscopy of free radicals and of radical containing entrance-channel complexes embedded in superfluid helium nanodroplets is reviewed. The collection of dopants inside individual droplets represents a micro-canonical ensemble, and as such each droplet may be considered an isolated cryo-reactor. The unique properties of the droplets, namely their low temperature (0.4 K) and fast cooling rates ($\sim 10^{16}\,\mathrm{K\,s^{-1}}$), provide novel opportunities for the formation and high-resolution study of molecular complexes containing free radicals. Radical production methods are discussed in the light of their applicability for embedding radicals in helium droplets. The spectroscopic studies performed to date on molecular radicals and on entrance/exit-channel complexes of radicals with stable molecules are detailed. The observed complexes provide new information on the potential energy surfaces of several fundamental chemical reactions and on the intermolecular interactions present in open-shell systems. Prospects for further experiments of radicals embedded in helium droplets are discussed, especially the possibility of preparing, studying, and manipulating high-energy structures, as well as the possibility of using them in fundamental physics experiments.

Contents

*Corresponding author. Email: jochen@fhi-berlin.mpg.de
†Current address: Emory University, Department of Chemistry, Atlanta, GA 30322, USA. Email: jeremy.merritt@emory.edu

International Reviews in Physical Chemistry
ISSN 0144–235X print/ISSN 1366–591X online © 2007 Taylor & Francis
http://www.tandf.co.uk/journals
DOI: 10.1080/01442350601087664

1. Introduction

Doped superfluid helium nanodroplets have emerged as a new and exciting tool for the study of the structure and dynamics of a quantum solvent as well as the embedded or attached atomic and molecular impurities themselves. The unique properties of the droplets, namely their low temperature and rapid cooling, make them a versatile tool for spectroscopic studies of metastable species. Although there have been a number of reviews on the spectroscopy of atoms and molecules embedded in or attached to helium nanodroplets [1–7], none of the articles cover the recent advances made in the study of open-shell, free radical metastable species. Therefore, an overview of this emerging field and the new possibilities it provides for the understanding of chemical reaction dynamics is timely.

Radicals and ions are among the most chemically reactive species known and play a key role in chemistry ranging from combustion processes [8] to the upper atmosphere [9] and molecular synthesis in the interstellar medium [10]. This high reactivity comes at a considerable cost to experimentalists; such transient species are often very difficult to maintain at sufficient concentrations to be probed experimentally.

While a great deal of progress has been made by isolating radicals in vacuum, much less is known about the interactions of radicals, or more generally, the features of their potential energy surfaces (PES). A focal point in chemical reaction dynamics has been to elucidate the properties of the transition state, the point on the PES where bonds are broken and reformed. Already in 1884 van't Hoff proposed an empirical, analytical expression for the rate constant of a reaction [11]. Five years later, Arrhenius provided a physical interpretation, relating it to an energy penalty needed to produce an *activated*

complex, which could then go on to produce the products [12]. A quantum-mechanical interpretation of the activation process was first given by London [13] and successively by Eyring and M. Polanyi [14], who introduced the concepts of a reaction path and the transition state as a saddle-point on a multi-dimensional PES (*Sattelgebiet des ,,Resonanzgebirges''*) for the $H + H_2$, $H + HBr$, and $H + Br_2$ reaction systems.† Later, rate constants and product state distributions could be qualitatively understood based on the form of the initial reagent energy (whether it be translational or vibrational) by developing the concept of early or late potential barriers [15, 16].

Recent experimental advances in reactive scattering have now enabled fully (initial and final) quantum state resolved reaction cross-sections to be determined for a few prototype systems, like $F + H_2$ [17–20], which was once considered to be the *holy grail* of the field. The matrix of initial and final quantum states provides a rigorous test of theoretical potential energy surfaces. One should note, however, that even at the full state to state level, impact parameter averaging acts to convolute the experimental results, sometimes making it difficult to draw quantitative conclusions on the detailed features of the potential. Furthermore, the scalability of such experiments to larger and larger systems is prohibitive. Oriented collisions [21–24], and especially the application of state-selected, decelerated molecular beams [25–29] and their use in scattering experiments [30] are likely to be important tools enabling the experimentalist to further reduce the effects of impact parameter averaging.

While reactive scattering is a sensitive probe of the repulsive wall of the PES, much less is known about the long-range dispersion forces between reactive species. Indeed, already Eyring and Polyani [14] discussed the additional effects of dispersion forces on the PES, which predicted a minimum for the symmetric H_3 molecule on their collinear PES. For the heavier systems they concluded that their calculations were not accurate enough to incorporate these effects quantitatively. The van der Waals minima lie at the base of the transition state, where the repulsive interactions balance dispersion,‡ and correspond to weakly bound clusters of two (or more) reactants or products. These species are called entrance or exit channel complexes, respectively. Given that the barriers to chemical reaction are typically several orders of magnitude larger than dispersion (van der Waals) forces, the importance of these van der Waals forces to reaction dynamics has largely been neglected. Recent experimental and theoretical work on the $Cl + HD \rightarrow HCl\,(DCl) + H\,(D)$ reaction, however, has shown that the corresponding orientational effects of the long range potential can strongly influence the branching ratios and the final state distributions by giving the reactants a torque, towards or away from the transition state [31–35]. Therefore, the long-range van der Waals forces can no longer be neglected for obtaining really quantitative results. For collisions at even lower temperature [30] such effects will be even more important. Moreover, also for the dissociation of formaldehyde [36, 37] and the hydrogen abstraction from hydrocarbon molecules by chlorine [38] the effects of long-range van der Waals interactions have clearly been observed. Therefore, it must

† It is interesting to note that these studies – on systems which are quite similar to the X-HY systems described in section 4.1 – were performed at the Kaiser Wilhelm-Institut in Berlin-Dahlem, the predecessor of the Fritz Haber-Institut where this review was written.

‡ More generally the *change* of dispersion and repulsion must cancel, i.e. for some coordinate system R: $\partial E_{\text{dispersion}}/\partial R + \partial E_{\text{repulsion}}/\partial R = 0$.

be concluded, that a quantitative understanding of van der Waals wells of molecular complexes is imperative.

One of the legacies that Roger Miller has left with us is the sensitivity of high-resolution spectroscopy of such weakly bound complexes as a probe of the surrounding PES. Here again, theory plays a crucial role in solving the multidimensional problem standing between the PES and the observed spectral transitions between eigenstates of the exact Hamiltonian. More recently, these spectroscopic techniques have been applied to reactive systems, where now the experimental methods have the added challenge of stabilizing the weakly bound complex and preventing the reaction. Sometimes the cooling provided by a free jet expansion is sufficient to stabilize such pre-reactive species, which can then be studied spectroscopically. The most common examples are X-HY complexes, where X is, for example, H_2 or a noble-gas atom, and HY is CH, OH, NH, SH, BH, or CN radicals. Many of the previous experiments have been performed using a noble-gas atom such as argon or neon to study the effects of dispersion, and in these cases no reaction can occur [39, 40]. Complexes have also been observed between reactive partners such as, for example, OH+CO [41], OH+H_2 [42–46], and CN+H_2 [47–50]. For these systems the barriers to reaction are still quite large: $\sim$17 kJ mol^{-1} for CN+H_2 [51] and $\sim$25 kJ mol^{-1} for OH+H_2 [52, 53]; the barrier for OH+CO is only $\sim$5 kJ mol^{-1}, but experiments are dominated by vibrational predissociation to the reactants [41]. So far these experimental techniques have relied on the exquisite sensitivity of laser induced fluorescence double-resonance methods in order to measure the spectra, which limit the choice of chromophores.

Many transient radicals have also been studied in solid noble-gas matrices [54–56]. Indeed, the inert matrix can be used to keep the radicals from interacting with one another, and in general the number of radicals can be built up using long deposition times. One can also raise the temperature of the solid matrix, which gives the dopants some mobility, eventually initiating reactions. Due to the large matrix effects, however, the spectra are often strongly perturbed, thus limiting the amount of information which can be extracted. Indeed, the highly anisotropic interaction is found to quench the free rotation of most molecules. In contrast to the more classical cryogenic matrices described above, cold, solid para-hydrogen matrices have also recently been used to study molecules in a more soft, quantum mechanical matrix [57–59]. Reactions of embedded impurities with H_2, the matrix material itself, can easily be studied, but the matrix is not as inert as noble-gas environments, as reactions of transient species with H_2 will typically occur [60].

Liquid helium nanodroplets combine many advantages of both types of solid matrix environments. They are inert due to the very noble, unreactive character of the helium atoms constituting the matrix and they perturb embedded impurities only very weakly due to their quantum-fluid nature, which manifests itself in the superfluidity of the droplets [61]. The droplets provide a very low ambient temperature of approximately 0.37 K, due to evaporative cooling and the low binding energy of helium atoms to the droplet. Molecules embedded in ^{4}He droplets show free rotation [62]. The formation of weakly bound molecular complexes inside helium nanodroplets proceeds through unique growth dynamics which are mainly determined by long-range forces between the complexation partners [1]. Therefore, often metastable clusters are stabilized and can be studied in the droplets [63, 64]. Additional information

on the PES can be obtained using infrared-infrared double-resonance spectroscopy, where the photo-initiated annealing of complexes provides branching ratios between different minima, limits on the barrier heights, and allows one to observe the products of photo-initiated chemical reactions [65, 66].

Extending such studies to transient, reactive species can provide novel materials, that can be studied using high-resolution spectroscopy. It should be possible, for example, to build linear chains from polar radicals just as in the case of HCN molecules [63]. Such systems are ideal candidates for chemical energy storage and provide large energy-to-mass ratios. The details of such prospective experiments are discussed in section 6.1. Moreover, the spectroscopic study of such highly energetic systems should provide complementary information to scattering experiments on chemical reaction dynamics.

In this review we will detail the experimental methods for embedding and studying radicals solvated in superfluid helium nanodroplets. In the following section a general introduction into helium droplet experiments is given, followed by the details of radical production. Then we will describe the experiments on radical monomers (section 3) and on radical-molecule van der Waals complexes in section 4. Afterward, a discussion of molecule-droplet interactions, emphasizing the additional information gained from spectroscopy of open-shell systems embedded in helium droplets (section 5), and an outlook for further applications (section 6) are given.

2. Experimental methods

2.1 *Spectroscopy in superfluid helium nanodroplets*

The experimental details concerning the production of neat and doped helium droplets have been given in previous reviews [1–6] and their thermodynamic properties have been discussed [67–69]. Therefore, here we will only discuss the relevant details and specialties for embedding radicals in the droplets. A schematic of the first apparatus for infrared spectroscopy of radicals embedded in helium droplets [70], built at the University of North Carolina at Chapel Hill (UNC), is shown in figure 1. In brief, the setup consists of a continuous helium droplet beam source and several, differentially pumped vacuum chambers. The source chamber contains the supersonic droplet beam source. The droplet beam passes through a skimmer into a region with a series of load lock ports to introduce pick-up sources of varying nature. After the droplets are doped they fly into a laser excitation region, where a multipass cell, consisting of two plane, parallel, gold-coated mirrors, is used to increase the interaction between the laser and the droplet beam. This spectroscopy region also has a pair of parallel electrodes, providing homogeneous fields up to $80\,\mathrm{kV\,cm^{-1}}$, in which Stark and pendular spectroscopy [71] can be performed. In all experiments reported here, the electric field is parallel to the laser-polarization, yielding $\Delta m = 0$ selection rules for the associated Stark and pendular spectra. The overall kinetic energy of the beam is then detected further downstream by a cooled semiconductor bolometer detector [1]. Alternatively, mass-spectrometric detection has been used in similar ways [1, 2], however, in that

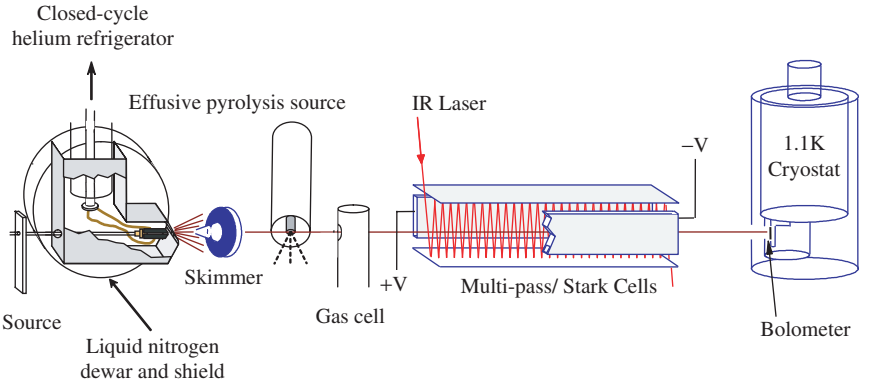

Figure 1. [Colour online] Experimental setup at UNC for the infrared spectroscopy of radicals in superfluid helium droplets; see text for details.

case the laser beam is typically sent collinear to the droplet beam to achieve sufficient signal to noise ratios.

Droplets are typically produced by expanding high-pressure helium (20–100 bar) through a small, cooled pinhole (5–10 μm, 5–30 K), as originally demonstrated by Becker *et al* in 1961 [72]. Droplets are formed in the early, high-pressure portion of the expansion and then successively cool by evaporation. In the case of ^{4}He, as used in all spectroscopic studies on radicals embedded in helium droplets so far, the evaporation temperature converges at ~ 0.37 K [67] and ^{4}He droplets exhibit superfluidity under these conditions [61].

Atomic and molecular *impurities* are embedded in the droplets by pick-up in scattering regions [1, 2]. The pick-up process is sequential, that is, individual atoms and molecules are picked up from the scattering gas, where only low densities are necessary, because the pick-up probability is determined by the large, geometrical cross-sections of the droplets. The cooling of dopants inside the helium droplet occurs on a timescale considerably faster than the complexation of multiple embedded species. For $(HCN)_n$ complexes embedded in a single droplet, for example, about $1000\,cm^{-1}$ of binding energy is released upon addition of each additional HCN molecule. If that energy would be deposited in the molecular complex, the cluster would anneal to its global minimum cyclic structure. However, the helium removes the energy quickly as the complex is forming and all modes orthogonal to the reaction path can be considered at their zero-point level. In the gas-phase the energy released along the reaction path has to be compensated by an increase in kinetic energy, i.e. the collision partners speed up. Inside a helium droplet, however, the energy is continually extracted by the helium and the molecules approach each other at minimum internal energy and relative velocity. Therefore, the complexes are often trapped in local minima and metastable species can be observed [63, 64]. Moreover, since the pick-up can be performed in multiple separate scattering regions, considerable control over the formation of larger clusters can be achieved, as, for example, shown for HF-Ar_n complexes [73]. This separable pick-up also allows one to produce clusters with quite complex compositions, possibly containing multiple species, and to embed species

under quite different conditions into the droplet. For example, thermally labile bio-molecules and metal atoms from a hot oven or radicals from an 1800 K pyrolysis source can be embedded in the same droplet, because the two species only come together in the cold confines of the droplet. This unique production process allows one to specifically design desired complexes inside helium droplets.

All molecular radicals or radical-molecule complexes embedded in a helium droplet that have been studied using high-resolution spectroscopy so far have either been stable molecules, like NO, that were picked up in an ordinary scattering chamber, or were produced in a continuous effusive pyrolysis source developed some years ago [70]; see section 2.2 for details.

Different detection schemes used in helium droplet spectroscopy have been described before [1, 2]. In all studies described in detail in this review, infrared depletion spectroscopy is used, where the evaporation of helium atoms from the droplet due to resonant infrared excitation of the dopant is detected [1]. In most of the studies reported here the reduced total kinetic energy of the droplet beam on a 1.1 K bolometer is measured using lock-in techniques, but mass spectrometric techniques, albeit less sensitive, have also been employed in infrared [1] and electronic spectroscopy [2, 7] of doped helium droplets. Bolometric detection is universal; evaporation of helium atoms from the droplet can be monitored but also excess vibrational energy transferred to it from the excited chromophore can be measured if the vibrational relaxation time is longer than the flight time of the droplets through the experiment [74, 75]. Due to its quasi-continuous operation mode the bolometer matches the continuous droplet beams very well and provides optimal experimental duty cycle.

In the interpretation of rotationally resolved spectra of species embedded in helium droplets the *matrix effects* of the droplet environment needs to be considered. Vibrational frequencies of the embedded molecules are typically shifted less than 0.1% from their gas-phase values, and due to the superfluidity of the droplets, free rotation of the embedded species can be observed [62]. The obtained rotational constants, however, are reduced from their corresponding gas-phase values [1, 62] and the influence of the droplet environment on the electronic structure can also be considerable. These effects are discussed in section 5.

2.2 *Radical production*

Some molecular radicals are relatively unreactive and can be bought and stored under ambient conditions. Therefore, a simple pick-up cell can be used to embed these species in the droplets. NO is an example of such a molecule that has also been studied in helium droplets [76].

For transient species, however, one has to resort to *in situ* methods of producing the radicals in the experiment. Several different methods for producing radicals for molecular beam studies have been developed, including pyrolysis, radio-frequency or microwave discharges, corona discharges, and photolysis [77, 78]. The most popular sources for use in combination with the extreme cooling provided in supersonic jet experiments are flash pyrolysis [79–81], electric discharge [82–84], and photolysis [85–87]. These methods are, however, not currently generally applicable for embedding molecules into helium droplets, as they are mostly operated in a pulsed fashion and

require relatively high gas pressures. While these radical sources are efficient in producing a large number of radicals, especially the discharge and photolysis sources often produce a large number of by-products. For gas-phase studies this does not necessarily represent a problem as long as the background pressure is kept low enough to prevent collisions, and that the target-radical concentration is high enough for the experimental sensitivity. Also, if a precursor or decomposition product absorbs in the same spectral region as the species of interest, then it may be difficult to separate out the overlapping bands. In a helium droplet experiment, however, all species are picked up by the droplets without any discrimination, giving rise to unwanted higher order complexes. Therefore, extremely clean sources of radicals, operating at low pressures, are required for these experiments in order not to contaminate all droplets. This includes buffer gas, which makes up most of the gas-phase expansion. Moreover, most helium droplet experiments today are operated as continuous beams and are therefore most efficiently used with continuous doping methods. Coupling pulsed radical sources to these beams, especially photolysis sources using intense pulsed lasers operating at 10 Hz, leads to large reductions of duty cycle and correspondingly lower signals. Once pulsed helium droplet sources are more widely applicable [88, 89], however, they may make such radical sources more compatible.†

2.2.1 Pyrolysis. The ideas from flash pyrolysis [79–81] can be transferred to conditions suitable for embedding radicals in helium droplets [70]. A scheme of the low-pressure, continuous, effusive pyrolysis source used at UNC is shown in figure 2. The source can routinely be heated to 1800 K to produce clean effusive beams of radicals from appropriate precursor molecules. Due to the optical transparency of liquid helium over an extremely wide energy range (up to 21 eV), black-body radiation from the hot source does not effect the droplet beam.

2.2.2 Other schemes. While our approach has been to generate the radicals externally and dope them into the droplets, another approach would be to produce radicals from photolysis of a stable molecule already embedded inside a helium droplet. Near threshold photo-dissociation of NO_2 in a helium droplet has been attempted with the goal of observing the NO-O radical-radical van der Waals complex, but this has not been successful [90–92]. It is unclear whether the helium is able to quench the energy faster than the time necessary to break the molecule apart, or the two fragments always react to give back NO_2. Braun and Drabbels [93] have used 266 nm photodissociation of CF_3I and CH_3I embedded in helium droplets to study the translational dynamics of the recoiling CH_3 (CF_3) and I atom fragments. Here, 266 nm photolysis promotes the CH_3I to a highly repulsive electronic state, which is known to dissociate very rapidly in the gas-phase [94]. In the helium droplet study gas-phase fragments ejected from the droplets were detected by velocity map imaging [95] and their product

† Commercial atom sources provide so-called *clean* atomic beams, but for the purposes of the experiments described here the atom-content is still too low. Initial experiments by ourselves to use microwave discharge sources were not successful due to the necessary low gas flow and pressure, in order not to destroy the helium droplet beam by a gas-jet from the discharge source.

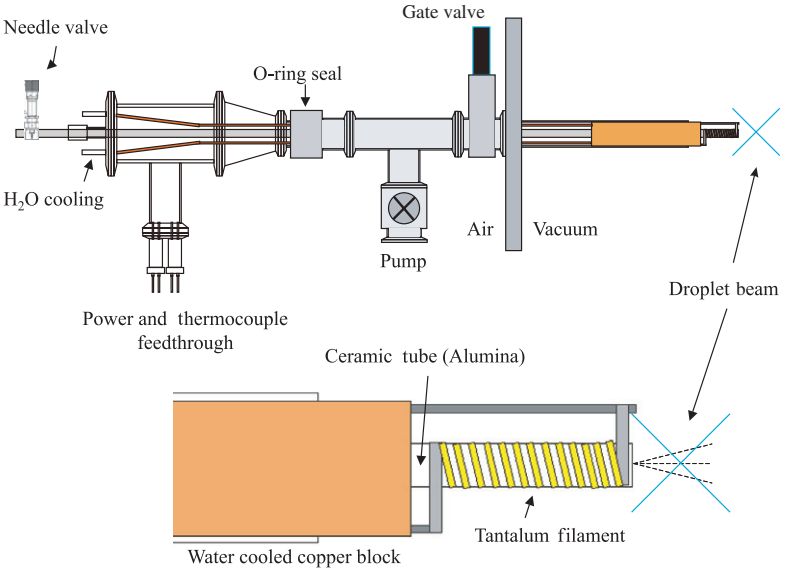

Figure 2. [Colour online] A schematic diagram of a pyrolysis source that can be load-locked into the helium nanodroplet apparatus, to facilitate the easy change of pick-up sources. In this case, an alumina tube is heated by a tantalum filament. A needle value is used to regulate the flow of the precursor through the source.

distributions were found to be less anisotropic and shifted to lower velocities than compared to the equivalent gas-phase experiment, consistent with a model of hard sphere collisions [93]. Since the detection method was based on imaging the gas-phase recoil products, studies were carried out using relatively small droplets, which allowed the fragments to escape. Photolyzing the embedded precursor in a much larger droplet, however, could allow one or both of the products to stay within the droplet.

Cold ion–molecule reactions have also been observed in helium droplets [96]. In this study 80 eV kinetic energy electrons were used to bombard the helium droplets, resulting in ionization of a single He atom in the droplet. The molecular impurity may then be ionized after resonant charge transfer [97]. Although the newly formed molecular ions are ejected from the droplet due to the energy released in the charge transfer step, ion–molecule reactions between these secondary molecular ions and additional molecules embedded in the droplet could be observed, yielding, for example N_2D^+ (from N_2^+ and D_2), CH_4D^+, or $CH_3D_2^+$ (from CH_4^+ or CH_3^+ and D_2) [96].

3. Radical monomers in helium droplets

3.1 *Propargyl*

The first spectroscopic study of a molecular radical in helium droplets was performed on propargyl (2-propynyl, C_3H_3) just five years ago [70]. In light of its role in sooting flames, the propargyl radical has been the focus of particular experimental attention [98–101]. Propargyl is one of the simplest conjugated systems with an odd number of

electrons, also making it the focus of considerable theoretical study [102–105]. There is compelling evidence that propargyl is the most important radical precursor in the formation of benzene, polycyclic aromatic hydrocarbons, and soot in certain combustion processes [98–101, 106–111]. For example, the simple dimerization of two propargyl radicals is thought to be important in the formation of benzene, as suggested by Wu and Kern [106].

The work on the transient and very reactive propargyl radical embedded in helium droplets demonstrated how to couple our continuous, low-pressure pyrolysis source to a helium droplet beam [70]. From a fit of the rotationally resolved infrared spectrum of the ν_1-transition the molecular parameters given in table 1 are obtained. We find that the $K_a = 1$ states are populated due to nuclear spin statistics, confirming the C_{2v} symmetry of this radical. This shows, moreover, that the local environment inside the helium droplet does not lower the symmetry. Indeed, nuclear spin conversion processes are extremely slow in the gas-phase [115], but even the presence of the unpaired electron and the collision rich condensed phase environment inside the droplet does not induce any noticeable spin relaxation on the timescale of the experiment (~ 1 ms), demonstrating the weak perturbation of the embedded radical by the helium droplet environment. Nuclear spin relaxation was observed in quantum-solid para-hydrogen matrices on a much longer timescale of minutes to hours [116] and the accelerating effect of added ortho-hydrogen was clearly observed. Since the ensemble of complexes studied in a helium droplet experiment is only from droplets with exactly the desired composition and the helium–complex interaction is generally weaker then the solid-hydrogen–molecule interaction, one would expect the conversion to be even slower in helium droplets.

While the A rotational constants of propargyl cannot be determined from the experimental data, the $(B + C)/2$ inertial parameters for ground and excited vibrational state were about one third of the gas-phase values, a reduction that is typical for rotational

Table 1. Summary of the molecular constants for the propargyl radical in superfluid helium droplets [70], compared to those obtained in gas-phase studies [112–114]. Numbers in parenthesis are one standard deviation.

Constant	Helium droplet[1]	Gas-phase[2]
A'' (cm^{-1})	9.60847[3]	9.60847 (18)
$(B'' + C'')/2$ (cm^{-1})	0.1198 (5)	0.312386 (12)
$B'' - C''$ (cm^{-1})	0.035 (2)	0.0105762 (35)
Δ''_N (cm^{-1})	0.00042 (1)	$7.35(122) \cdot 10^{-8}$
A' (cm^{-1})	9.60258[3]	9.60258 (11)
$(B' + C')/2$ (cm^{-1})	0.1185 (5)	0.311641 (7)
$B' - C'$ (cm^{-1})	0.035 (2)	0.010496 (13)
Δ'_N (cm^{-1})	0.00062 (1)	$5.37(76) \cdot 10^{-8}$
ν_0 (cm^{-1})	3322.15 (1)	3322.292 (10)
μ''_a(D)	−0.150 (5)	–
$\Delta\mu_a$(D)	0.02 (1)	–

[1]Reported helium droplet values are from reference 70. The values for $B - C$ were mistyped in the original publication and the corrected values are given here.
[2]Reported ground state values are from reference 112, excited state values are from reference 113.
[3]A'' and A' are fixed at their respective gas-phase values.

constants of this size [1]. The asymmetry-splittings $B - C$ are increased in the helium droplet environment, probably due to differential effects of the helium droplet environment on the rotation around the different axes.

This study was the first to experimentally determine the permanent dipole moment of the propargyl radical by measuring the rotationally resolved infrared spectrum in the presence of a strong homogeneous electric field ($50\,\mathrm{kV\,cm^{-1}}$). It is known that dipole moments determined by Stark spectroscopy in helium droplets are very comparable to the gas-phase values [117]. This is confirmed by the good agreement of the measured ($\mu_0 = -0.150(5)$ D and the $\Delta\mu_{v=1\leftarrow 0} = 0.02(1)$ D) and calculated ($\mu_e = -0.14(3)$ D, $\mu_0 = -0.124$ D, $\mu_{v=1\leftarrow 0} = 0.011$ D) values for propargyl [103, 118].

3.2 *Nitric oxide*

Recently, the nitric oxide (NO) radical was studied using infrared diode laser spectroscopy in helium droplets [76]. Only the $Q(1/2)$ and $R(1/2)$ transitions of the $v = 1 \leftarrow 0$ transition in the $^2\Pi_{1/2}$ electronic ground state were observed due to the low temperature (0.4 K) of the droplet and the small moment of inertia of NO. From the line separation the rotational constant of NO in helium droplets is measured to be $B = 1.253\,\mathrm{cm^{-1}}$, which is 76% of the gas-phase value, in good agreement with previous closed-shell systems of this size.

For the $Q(1/2)$ line sharp transitions are obtained. This reflects the fact that vibrational relaxation is slow due the absence of low-lying vibrational modes [75, and references therein]. Indeed, previous studies of HF embedded in helium droplets have shown that the monomer does not vibrationally relax on the timescale of the experiment (~ 1 ms) [74], so instead of depleting the droplet beam intensity, the extra vibrational energy of HF is simply carried to the bolometer. Using a mass-spectrometer based detection scheme, such as that used in the study of NO, one would not *a priori* expect a depletion signal in this case. Molecular absorption beam depletion can still be detected, however, due to pick-up of an impurity, i.e. a second NO or N_2, after the infrared excitation, leading to relaxation of the vibrationally excited molecular dimer, as shown conclusively for HF [75]. The resulting long monomer lifetime allows the nuclear hyperfine and Λ-doubling splittings of the transition to be resolved. The nuclear hyperfine splitting is unchanged from the isolated gas-phase value, whereas the Λ-doubling is increased by a factor of 1.55 compared to the gas-phase [76]. Von Haeften *et al*. discuss this effect in terms of electronic coupling and also suggest the possible influence of the helium density around the NO molecular axis [76]. For more details of these effects see the results on the NO-HF complex in section 4.3 and the general discussion of molecule-droplet interactions in section 5.

The $R(1/2)$ line of NO in helium droplets, on the other hand, shows a single unresolved band that fits well to a Lorentzian lineshape, which is attributed to fast rotational relaxation in the vibrationally excited state with a lifetime of 1.52×10^{-10} s. The large rotational constant of NO places the excited rotational state in a region of high density of states for the fundamental excitations of the droplet, leading to a strong coupling and the corresponding short lifetime [1].

The NO molecule was also used as a sensitive probe of electronic effects of molecule-droplet interactions [119]. In that study, NO embedded in liquid helium droplets was

photoionized and the ongoing dynamics was found to be quite complex. NO is initially excited by a two-photon excitation from its $^2\Pi$ electronic ground state to low-lying Rydberg states (NO*). Subsequently, the nuclear degrees of freedom in NO*, and the nuclear degrees of freedom between the NO* and the helium environment, relax, resulting in NO* being transported to the droplet surface on a timescale shorter than the laser pulse (< 10 ns). NO* can then leave the droplet, accompanied by a modest number of helium atoms or, alternatively, it can be photoionized on the surface of the droplet. NO^+ can then be resolvated, resulting in snowball formation [120–123] around the ion-core, or leave the droplet surrounded by helium atoms.

3.3 *Other species*

Several other radicals or transient species have been observed in or on liquid helium droplets. For example the spectra of individual open-shell metal atoms on the surface of helium droplets have been obtained [4, 7, 124–126] and the chemiluminescence emission spectrum of the BaO^* product from the reaction $Ba + N_2O \rightarrow BaO^* + N_2$ inside a helium droplet has been observed [127]. The reaction was found to proceed very efficiently inside the droplet, and the influence of co-embedded xenon clusters was studied, which showed that the xenon pulls the nascent BaO, initially formed at the surface, into the centre of the droplet. Experiments on the photodissociation of CF_3I to form CF_3 and I inside the helium droplets [93] and on ion–molecule reactions [96] were already discussed in section 2.2.

4. Radical-containing molecular complexes

Whereas the effects of the moderately strong long-range electrostatic interactions in ion–molecule reactions are well known to have a significant influence on the associated reaction rates [128, 129], the importance of the weaker van der Waals forces in the entrance channels of neutral reactions have only recently begun to be entirely appreciated [38, 41, 130, 131]. Experimental and theoretical work on the $Cl + HD \rightarrow HCl\,(DCl) + D\,(H)$ reaction shows that the torque experienced by the HD in the entrance valley of the PES has a significant effect on the overall reaction rates and branching ratios [32–35]. Furthermore, the rotational excitation of HCl products formed from abstraction reactions of chlorine and organic molecules, for example, can only be accurately described by taking into account the features of the exit channel. The dipole–dipole interaction of the departing fragments was found to be very important in determining the product final state distributions [38]. For the dissociation of formaldehyde a completely new dissociation mechanism (*roaming hydrogen atom* mechanism) has been proposed [36, 37]. These results are clear examples showing that entrance and exit channel complexes of molecular reactions probe the associated PES at energies that are relevant to the systems' chemical reaction dynamics, despite being much lower in energy than the corresponding transition states. This is due to the torque on the reactants at long range that acts to deflect trajectories towards or away from the transition state [34]. Therefore, these complexes are of considerable

importance in understanding the nature of the reactions, particularly at low translational energies (low temperatures).

The isolation and stabilization of entrance and exit channel complexes in liquid helium droplets and their high-resolution spectroscopic study provides a novel experimental approach for studying these important systems. In the remainder of this section we will summarize the experiments performed on such complexes in liquid helium droplets to date. In the first part we will discuss the hydrogen-bound complexes of halogen atoms with small linear molecules and in the second part of this section we will proceed to complexes of hydrocarbon radicals with Brønsted acids.

4.1 *Complexes containing halogen atoms*

Recently, a large series of complexes of closed-shell molecules with halogen atoms embedded in liquid helium droplets have been studied using high-resolution infrared spectroscopy, i.e. the complexes of chlorine, bromine, and iodine with HF and HCN, respectively [132, 133]. These systems represent the prototypical *heavy-light-heavy* X–HY (X = Cl, Br, I; Y = F, CN) complexes which serve as prominent benchmark systems for the understanding of elementary reaction dynamics studies. They can be studied in great detail theoretically [134–148], as they contain only two heavy atoms (X-HF) and only a few nuclear degrees of freedom. Some stationary points of such systems have also been studied experimentally, for example, by spectroscopy of the transition states [144, 149–151] and using infrared spectroscopy in noble-gas matrices [152–154]. These studies, however, did not reveal detailed information on the associated entrance or exit channel regions of the reactions.

The X-HF [155–160] and X-HCN [161–163] PES have also been studied in collision experiments. Recently, strong rotational enhancement has been described for the F + HCl reaction [160, 164]. The chemiluminescence from HF produced in chemical lasers, i.e. from reactions of ClF with hydrogen, has been observed [165]. However, so far no spectra of the stationary points on the PES have been obtained for the free molecular complexes.

For these X-HY systems, the interaction of the quadrupole moment of the halogen atom with the dipole moment of the molecule suggests two linear structures with the atom sitting on either end of the linear molecule [166, 167]. However, T-shaped minima are also predicted due to the considerable quadrupole moments of the molecules [134, 135, 140, 141, 143]. The weak interaction between a halogen atom and the molecules in a van der Waals complex suggests, that, to a first approximation, the orbital angular momentum λ_A of the atom will be conserved in the complex. This interaction removes the degeneracy of the ^2P atomic states, which in C_s symmetry gives rise to two states of A' and one state of A'' symmetry. These correspond to the three relative orientations of the singly occupied orbital with respect to the complexation partner, i.e. the unpaired electron being in the p_x, p_y, or p_z orbital, respectively. Solving for the eigenvalues of the electronic Schrödinger equation under the Born–Oppenheimer approximation yields the adiabatic PES. However, since these surfaces are coupled by non-adiabatic coupling terms originating from the nuclear kinetic energy operator, it is often helpful to solve for the bound states in a diabatic representation [135, 143]. The electronic anisotropy is further complicated due to

electron spin, and spin–orbit coupling can also have an important effect on shaping the PES. For comparison we reproduce the lowest diabatic and adiabatic PES including spin–orbit coupling for the Cl-HCl, Cl-HF, and Br-HCN complexes in figure 3(A–C), (D–F), and (G), respectively. The results for Cl-HCl [142, 143] and Cl-HF [146, 147]

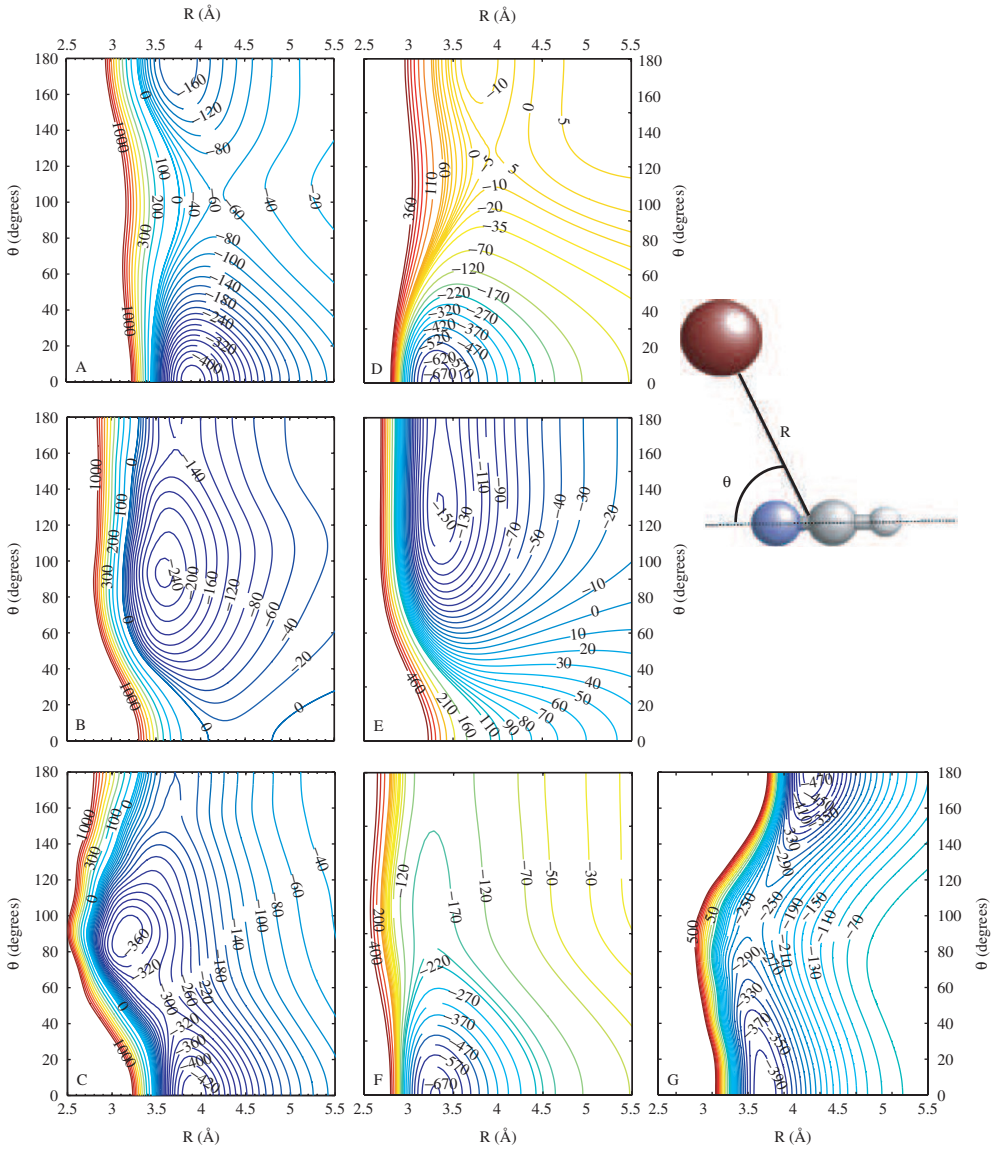

Figure 3. (A, D) Diabatic potential energy surfaces for Cl-HCl and Cl-HF $j_A = 3/2$, $\omega = 3/2$ and (B, E) $j_A = 3/2$, $\omega = 1/2$, respectively. (C–F) The lowest adiabatic potential energy surface including spin–orbit coupling for Cl-HCl (C), Cl-HF (F), and Br-HCN (G), respectively. Jacobi coordinates as shown in the inset have been used throughout and $\theta = 0$ corresponds to the hydrogen bound arrangement. See text for details.

have been published previously, while preliminary results for Br-HCN have been provided by van der Avoird. The general topology of the Cl-HCl and Cl-HF surfaces are quite similar. However, the larger dipole of HF, compared to HCl, makes the linear hydrogen bound minimum deeper for Cl-HF and the T-shaped minimum has almost completely disappeared in the lowest adiabatic surface. Indeed, for Cl-HF only the linear hydrogen bound isomer was observed experimentally in helium droplets, suggesting that the T-shaped or linear HF-X isomers are not formed. Detailed comparisons of the experimental and theoretical results for the X-HF systems have been given elsewhere [133, 141, 146, 147]. In contrast, the lowest adiabatic surface for the Br-HCN system shows two deep minima corresponding to the hydrogen-bound and nitrogen-bound linear isomers, respectively, which are both observed experimentally [132].

The $1\,^2A'$ and $1\,^2A''$ surfaces of Br-HCN are degenerate at the linear H-bound configuration ($\theta = 0$), whereas the $1\,^2A'$ and $2\,^2A'$ surfaces are degenerate at the linear N-bound configuration ($\theta = 180$). Therefore, the electronic symmetry is $^2\Sigma$ for HCN-X, with the unpaired electron along the axis of the molecule, and $^2\Pi$ for X-HCN, with the unpaired electron perpendicular to the axis of the molecule.

In figure 4 survey scans for the Br-HCN systems with cold (room temperature) and heated (~ 1600 K) pyrolysis source are shown as an example. Such overview scans are infrared depletion spectra obtained in the presence of strong homogeneous electric fields ($\sim 60\,\mathrm{kV\,cm^{-1}}$) in which the complete rotational structure is collapsed into a single *pendular transition* [71, 168, 169] due to the large degree of orientation of the polar molecules in the cold environment.

When the pyrolysis source is cold, only complexes of HCN with halogen molecules are formed. When the pyrolysis nozzle is heated, however, the signals associated with the precursor complexes are significantly reduced, due to the dissociation into atoms, and a new set of signals is observed to grow in, which are readily assigned to binary complexes of bromine atoms with HCN. Based on harmonic vibrational frequency

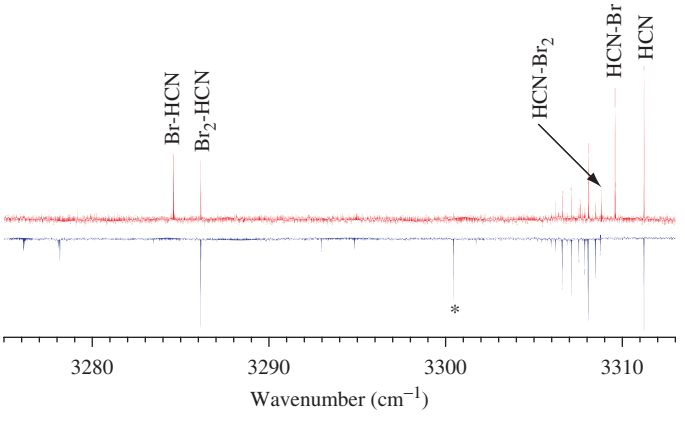

Figure 4. [Colour online] Pendular survey scans revealing the pyrolysis source temperature dependence (upward peaks are with a hot source, downward peaks are with a cold source) for the HCN + bromine experiment. The scans show peaks which we identify as molecular and atomic bromine complexed with HCN. The peak labelled with an asterisk is a known impurity.

calculations as well as physical intuition, the largely different frequency shifts of the ν_{CH} stretching vibrations result from the two different structures of the complexes, namely the peak shifted furthest to the red corresponds to the Br-HCN complex, and the peak which exhibits only a small shift is related to the HCN-Br complex. This assignment is confirmed by analysis of the field-free spectra of each of these transitions [132, 170].

In figure 5 the field-free spectrum of Br-HF is shown as an example. The vibrational frequency is shifted by 131 cm^{-1} to lower energy compared to the HF monomer transition [74], indicating the binding of Br to the hydrogen end of HF. The simulation of the rotationally resolved spectrum, constituted by all the individual simulated transitions shown at the bottom of the figure, reproduces all of the important features of the spectrum. Some deviations are observed especially for the lowest-J transitions, an effect that is regularly observed for molecules embedded inside helium droplets; see section 5 for details. The overall structure and all features are clearly reproduced by the simulation. Therefore, these spectra confirm the $^2\Pi_{3/2}$ ground states of these hydrogen bound complexes, consistent with the $^2P_{3/2}$ ground state of atomic bromine. Spectra and simulations of the same quality are obtained for all other hydrogen bound X-HF/HCN complexes studied. The molecular parameters obtained for the ground states for all complexes are given in table 2. In figure 6 the field-free spectrum of the nitrogen-bound HCN-Br complex is shown for a comparison. These nitrogen-bound complexes exhibit quite different features than the hydrogen bound complexes. Whereas the ν_{CH} vibrational frequencies are shifted by tens of wavenumbers for the hydrogen bound complexes, these N-bound complexes are shifted only by a few cm^{-1} compared to the free HCN molecule. The rotationally resolved spectra of

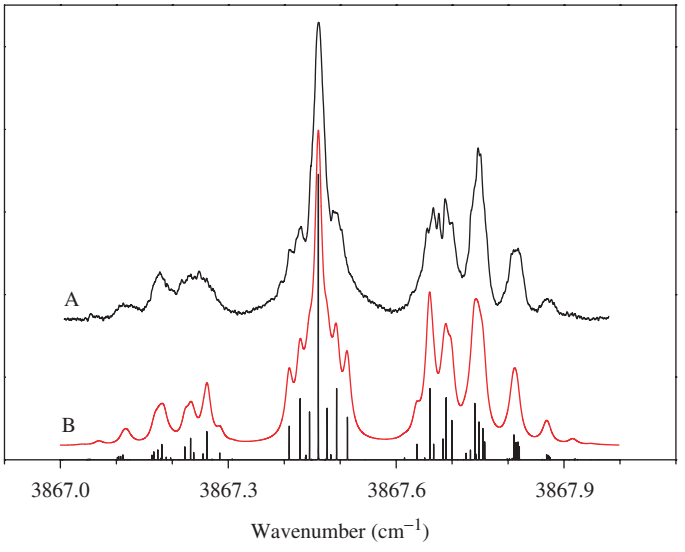

Figure 5. [Colour online] (A) The field-free infrared spectrum of Br-HF shown together with (B) a simulation that includes nuclear magnetic hyperfine interactions due to the bromine nucleus ($I = 3/2$). The stick spectrum shows all of the transitions that underlie the observed features.

the HCN-Br and HCN-I complexes also show a very different fine-structure, which we tentatively assign to parity splitting due to the spin–orbit interaction between the $^2\Sigma_{1/2}$ and the $^2\Pi_{1/2}$ states of the complex [132, 170], in agreement with recent theory for the HCN-Br system by van der Avoird's group [148]. For the HCN-Cl complex no such fine-structure could be observed, which is consistent with the much smaller spin–orbit coupling constant of atomic chlorine than for bromine and iodine, and the correspondingly small splittings of the transitions that are not visible at the resolution of our experiment.

It had been proposed that Cl-HCl complexes may posses T-shaped structures, but display several of the properties of a linear open-shell molecule [143]. Given the frequency shift from the HF monomer, however, this is unlikely the case for the X-HF complexes observed here; see reference [133] for a detailed discussion. Nevertheless, the fact that this point is subject of considerable debate illustrates how poorly we still understand these species, calling out for more experiments and theory on these entrance channel complexes.

No complexes of atomic fluorine with HF or HCN have been observed, despite extensive searches for such complexes and a previous assignment for the ν_{HF} stretching vibrations of F-HF in argon matrices [154]. Moreover, from *ab initio* calculations it is clear, that the reaction of F + HCN to form HFCN via an insertion mechanism is quite exothermic and exhibits only a small barrier or no barrier [132, 170]. The fact that the fluorine containing F-HCN complexes have not been observed, could be an indication that the insertion reaction takes place, even at 0.37 K. This reasoning is also supported by argon matrix work where the insertion product has been observed, whereas no pre-reactive (van der Waals) complexes were found [171, 172]. Guided by the experimental vibrational frequency of 3018 cm^{-1} for HFCN in solid argon, we also searched for the HFCN reaction product in the helium droplets. However, since

Table 2. Ground state molecular parameters from infrared spectroscopy for the complexes of HF and HCN with halogen atoms observed so far [132, 133]. For chlorine and bromine the constants of the lighter isotopologue are given (iodine has only a single isotope) and the isotope splittings are the frequency of the lighter isotopologue subtracted from the frequency of the heavier one.

Species	ν_0 (cm^{-1})	B^1 (cm^{-1})	D(10^{-4} cm^{-1})	μ (D)	$a\Lambda+(b+c)\Sigma$ (cm^{-1})	isotope splitting[2] (cm^{-1})	B_{gas}/B_{He}
^{35}Cl-HF	3887.54	0.055	1.2	1.9	0.005	0.038	2.3
^{79}Br-HF	3867.46	0.043	0.95	2.1	0.045	0.010	2.2
I-HF	3847.82	0.037	0.3	2.2	0.035	–	2.2
Br-HCN	3284.61	0.0151	1.5		0.04	[4]	2.7
I-HCN	3277.79	0.0120	1.0		0.04	–	2.83
HCN-Cl	3309.33	0.032	0.50	3.0	–	0.001[4]	2.7
HCN-Br	3309.55	0.019	0.12	3.78	–	[4]	2.75
HCN-I	3309.37	0.016	0.10	(3.91)[5]	–	–	2.75

[1]From references [132, 133].
[2]The frequency of the heavier complex subtracted from the corresponding one of the lighter isotopologue.
[3]Gas-phase values are from *ab initio* calculations [132, 133]. For the HCN-X complexes the gas-phase values are B_0 values from one-dimensionally spin–orbit corrected adiabatic PES [132].
[4]No isotope splitting is observed experimentally, which is consistent with bound state calculations on an one-dimensional *ab initio* potential energy surface for HCN-Cl; splittings for the bromine complexes are expected to be even smaller [132].
[5]*ab initio* value from reference [132].

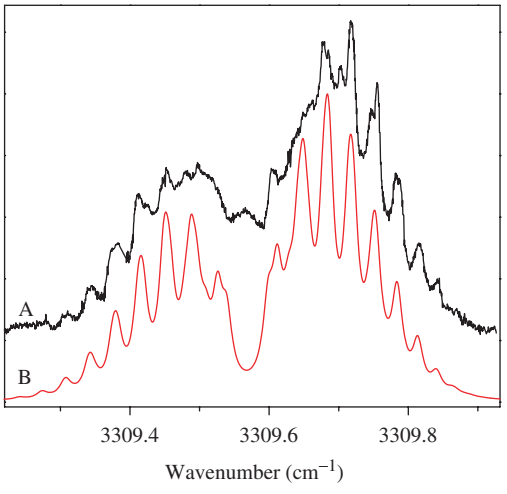

Figure 6. [Colour online] (A) The field-free infrared spectrum of HCN-Br shown together with (B) a simulation that includes parity splitting induced by spin–orbit coupling of the $^2\Sigma_{1/2}$ and the $^2\Pi_{1/2}$ states of the complex; see text for details.

this frequency is at the edge of the F-centre laser tuning range and the transition strength is about 50 times weaker than for the HCN monomer, no manifestations of the HFCN product could be observed. Revisiting the experiment using newer technology OPO lasers [170, 173, 174], which have enhanced tuning ranges and improved power, might reveal its spectral signature.

Similar studies to the ones described here have also been performed on the pre-reactive complexes of open-shell metal atoms (Al, Ga, In) [170] and semiconductor atoms (Ge) with HCN and preliminary results were presented in an earlier review [1]. Upon complex formation in liquid helium droplets the same linear van der Waals complexes as for the halogen atom HCN complexes are observed. However, these atom-HCN complexes can undergo an exothermic insertion reaction and the corresponding barriers are low enough that the reactions actually do proceed even at the low ambient temperatures of the helium droplet, depending on the metal, either directly or initiated by a single-quantum excitation of the ν_{CH} stretching vibration in the HCN moiety [1, 170, 175]. Details on the van der Waals complexes and the insertion products will be published elsewhere [175]. Furthermore, the complexes of HCN with several alkaline (Na, K, Rb, Cs) and alkaline earth (Mg, Ca, Sr) atoms [176, 177], Zn atoms [178], and Cu and Au atoms have been observed. The complexes of one to six magnesium atoms with several small molecules have been studied extensively [179–182]. Due to the electronic quasi-closed-shell structure of magnesium and high barriers to reaction in these systems, these complexes exhibit the simple spectra of closed-shell van der Waals complexes. For the heavier atoms from these series it is known that the atom resides on the surface of the droplet, forming a dimple [2, and references therein]. It is interesting to study the effects of embedding an atom that wants to stay on the surface of the droplet, and a molecule that wants to be inside the droplet, which, in addition, strongly attract each other.

For Na-HCN, one such system, a very strong absorption line is observed [176, 177]. The remaining rotational structure, however, resembles the spectrum of a linear or spherical top with a very much larger moment of inertia than that expected for a Na-HCN binary complex, even inside a helium droplet. Based on the observed scaling of the rotational constant with the droplet size, along with the very large reduction in B upon solvation in the droplet, Na-HCN is presumed to rotate about the surface of the droplet. The spectra of the heavier atoms (K, Rb, Cs, Ca, Sr) show similar effects; for some of them even both species can be observed simultaneously – an embedded van der Waals complex as for Mg-HCN and a surface-bound complex as for Na-HCN [176, 177].

4.2 *Complexes of hydrocarbon radicals*

4.2.1 Complexes of methyl radical with HF and HCN. The reactions of hydrocarbons are of particular interest due to the wide range of reactions for which they play a key role, for example combustion processes [8]. Their hydrogen exchange reactions with fluorine atoms form a basis of our understanding of much larger systems. The simplest fluorine + hydrocarbon system, $F + CH_4 \rightarrow HF + CH_3$, has been extensively studied both experimentally [183] and theoretically [184], however, high-resolution spectroscopic studies of the entrance and exit channel regions of the PES are still lacking. Previous studies have identified the CH_3-HF complex in argon matrices [54, 185–187].

In order to probe the exit channel region of the PES, methyl radicals have been produced via pyrolysis, while a second pick-up cell was used to dope the droplet with an HF molecule. Azomethane, di-tert-butyl peroxide (DTBP), and CH_3I were all used as precursors for CH_3 to confirm that the signals genuinely arose from CH_3. In addition, several transitions of the CH_3 monomer were also observed in helium droplets. Figure 7(A) shows a partially rotationally resolved experimental spectrum which is assigned to the HF stretching vibration of the CH_3-HF molecular complex. The C_{3v} symmetry of the complex can be uniquely identified from the large Q branch present in the spectrum. Indeed, at the temperature of the droplets, we would not normally expect population of the excited K states since the rotation about the *a*-axis only moves the three hydrogen atoms, giving rise to a large energy spacing between different *K* states. Assuming nuclear spin conversion is slow compared to the timescale of the experiment, the $K = 0, 3, 6 \ldots$ and $K = 1, 2, 4, 5, 7 \ldots$ states are separate identities of *A* and *E* symmetry, respectively, with respect to the the nuclear spin statistics of the rovibrational wavefunction; thus they do not interconvert upon cooling to 0.37 K. At the temperature of the droplets, all of the population is cooled into the $K=0$ and $K=1$ states. $\Delta J = \pm 1$ transitions are allowed for both *K* manifolds, but $\Delta J = 0$ transitions are only allowed for $K=1$ states. The intensities reflect the population of $A:E$ states of CH_3 in the high-temperature source, yielding a $\sim 1:1$ population ratio for the $K=0$ and $K=1$ bands.

The linewidths in the CH_3-HF spectrum are rather broad, somewhat limiting the accuracy of the molecular parameters determined by the fit to the spectrum, shown in figure 7(B)–(D). The broadening suggests a vibration-vibration resonance as the cause of the shortening of the excited state lifetime, arising from coupling the HF

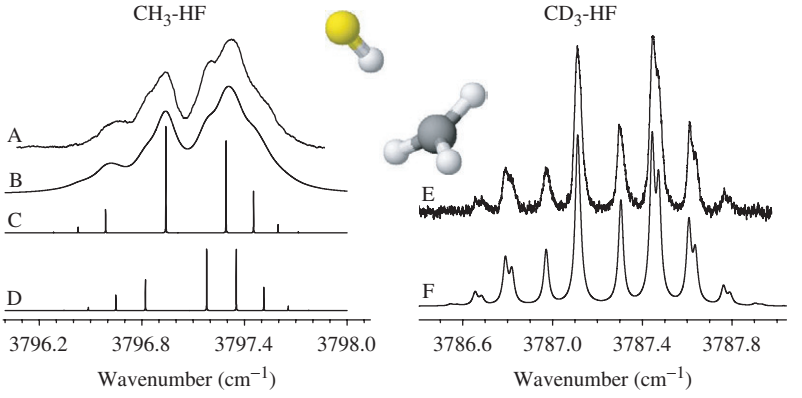

Figure 7. [Colour online] (A) An experimental spectrum corresponding to the HF stretching vibration of the CH_3-HF molecular complex, along with a symmetric top simulation (B) which clearly shows the C_{3v} symmetry of this complex. In (C) and (D) we plot the contributions from the $K = 1$ and $K = 0$ bands, respectively, illustrating that nuclear spin symmetry prevents interconversion of these two manifolds of states. Scan (E) shows the corresponding spectrum for CD_3 radicals, with the substantially narrower lines illustrating a dramatic increase in the lifetime of the complex and (F) the corresponding simulation.

stretch excited state to the CH_3 stretches of the methyl radical within the complex. To test this idea, we also recorded the spectrum of CD_3-HF, which is shown in figure 7(E). CD_3 radicals were produced by pyrolysis of CD_3I. Deuteration of CH_3 lowers the frequencies of the vibrations as shown in figure 8, detuning the resonance, and resulting in much narrower lines, corresponding to a longer lifetime. The molecular parameters derived from the fits to the spectra are summarized in table 3.

In addition to the importance of the long-range van der Waals forces in giving the reactants a torque, which may be towards or away from the transition state [31–35], the stabilization of weakly bound reactive complexes may represent an ideal starting point for the study of reactive resonances [19]. The experimental observation of reactive, or Feshbach, resonances in chemical reactions are highly sought because they result from purely quantum mechanical effects and probe regions of the PES which are not sampled by typical experimental techniques. Such reaction resonances result from a coupling to vibrationally adiabatic wells near the transition state, giving rise to dynamical trapping [19]. Reactive resonances have been confirmed in the crossed molecular beam reactive scattering of $F + H_2 \rightarrow HF + H$ [19] and the photo-electron spectrum of IHI^- [191]. Resonances of this type are not expected to be constrained to such simple systems, it is only our ability to detect or recognize them, which has limited current experiments to such simple systems. Only recently has a reactive resonance been implicated in a true polyatomic reaction, namely $F + CH_4 \rightarrow HF + CH_3$ [183]. At low collision energies the transient resonance in this reaction can proceed via predissociation into $HF(v = 2, j') + CH_3(v = 0)$, similar to F + HD [19]. The extra degrees of freedom of the CH_3, however, may allow intramolecular vibrational energy redistribution (IVR) which would shorten the resonance lifetime, allowing the $HF(v = 2) + CH_3(v_1 = 1)$ IVR channel to compete effectively with the

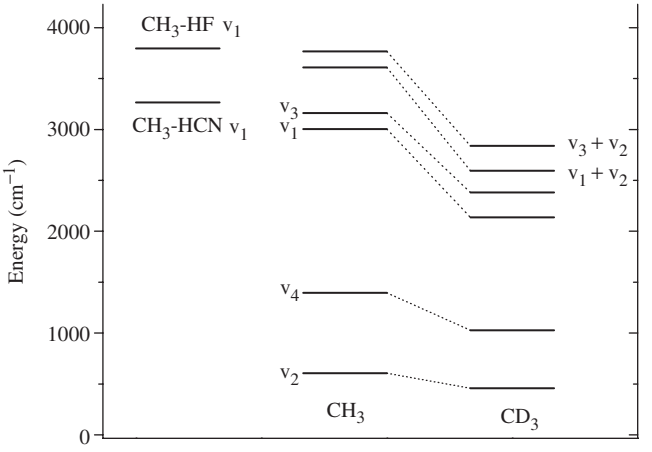

Figure 8. A plot of the experimental excitation energies of the CH_3-HF [188] and -HCN complexes [189] and of the different vibrations in the CH_3 and CD_3 monomers [190]. The effect of deuteration in the CD_3-HF complex is to lower the vibrational frequencies of the CH stretches, effectively quenching the vibration-vibration resonance that occurs with the excited HF stretching state of the complex. See text for details.

Table 3. Ground state experimental molecular constants of hydrocarbon-HF and -HCN complexes. Comparison to *ab initio* inertial parameters shows reduction factors for the rotational constants as for closed-shell systems of the same size [1].

Species	ν_0 (cm^{-1})	A (cm^{-1})	ΔA (cm^{-1})	$(B+C)/2$(cm^{-1})	D_J(cm^{-1})
CH_3-HF	3797.00		0.06[1]	0.09	$2.5 \cdot 10^{-4}$
CD_3-HF	3787.14		0.027[1]	0.083	$2.6 \cdot 10^{-4}$
C_2H_5-HF	3774.45	0.30		0.059	$4.8 \cdot 10^{-5}$
C_3H_5-HF	3810.10	0.095		0.040	$1.0 \cdot 10^{-4}$
CH_3-HCN	3265.70		0.04[1]	0.030	$3.7 \cdot 10^{-5}$
CD_3-HCN	3262.09		0.018[1]	0.027	$2.6 \cdot 10^{-5}$
C_2H_5-HCN	3260.29	0.30		0.15	$2.9 \cdot 10^{-5}$
C_3H_5-HCN	3260.14	0.09		0.016	$8.0 \cdot 10^{-6}$

[1]These parameters are taken from gas-phase work [54, 185].

pre-dissociative decay described above. At higher collision energies the decay of the resonance state into $HF(v=3) + CH_3(v=0)$ dominates [183].

From our experiments on the CH_3-HF and CD_3-HF complexes we can confirm a similar coupling between ν_{HF} and $\nu_{combination}$, the states of the complex corresponding to $HF(v=1) + CH_3(v_1=0)$ and $HF(v=0) + CH_3(v_1=1)$, respectively, as indicated by the IVR-limited excited state lifetime, which is considerably lengthened in the case of CD_3-HF. Overtone pumping of the CH_3-HF van der Waals complex may allow access to the region of the PES directly involved in the reactive resonance, as proposed for $F + H_2$ [19].

In order to further explore the *v*-*v* coupling mechanism observed for the CH_3-HF complex, one can also alter the energy of the bright state by changing the identity of the chromophore. Rotationally resolved infrared spectra have been recorded for

the CH_3-HCN and CD_3-HCN complexes [189]. As seen from the energy level diagram in figure 8, the CH stretching frequency of HCN in the complex lies below the combination levels of the CH_3 monomer, implicated in the relaxation of CH_3-HF, so a more direct comparison of the coupling can be made with just the ν_1 and ν_3 levels of CH_3. Interestingly for CD_3-HCN, the combination band for CD_3 is a viable relaxation channel. The peaks in the CH_3-HCN spectrum are well fit by a Lorentzian lineshape, just as in CH_3-HF, suggesting that the broadening results from the finite lifetime of the excited state. Comparing the observed linewidths for CH_3-HCN and CH_3-HF we find that the lifetime of CH_3-HCN is approximately two times longer than for CH_3-HF, suggesting that the coupling to the combination band is indeed the important relaxation channel for CH_3-HF. The CD_3-HCN molecular complex exhibits linewidths which are only slightly smaller than for CH_3-HCN, clearly showing that the effect of coupling to the CH stretches of the CH_3 directly is much smaller.

To our knowledge no studies have investigated the possibility that combination modes are excited in the F+CH_4 reaction, other than pure overtones. Based on our observed vibrational coupling of the $HF(v = 1) + CH_3(v = 0)$ to $HF(v = 0) + CH_3(\nu_1 = 1 \text{ or } \nu_3 = 1 + \nu_2 = 1)$ states of the complex, it may be possible to observe this reaction channel in an crossed molecular beam reactive scattering experiment similar to the ones reported by the group of Kopin Liu [183, 192], where the experimental conditions favour the production of methyl in the CH-stretch excited state, i.e. near threshold.

4.2.2 Larger hydrocarbon radicals. Larger hydrocarbon radicals, including ethyl (C_2H_5) and allyl (C_3H_5) radicals, may be readily formed by pyrolysis of their corresponding iodine precursors [79, 193–195], and spectra have been recorded for their complexes with HCN and HF embedded in helium droplets. These systems are of interest since they may be directly compared with the methyl radical complexes observed previously. Figure 9 shows a pendular survey scan for the HF stretching region. In the bottom trace C_2H_5I is flowed through a room temperature pyrolysis source, and the peak at $3747\,cm^{-1}$ is assigned to a C_2H_5I-HF complex. Upon heating the source, this peak is observed to decrease in intensity, and a new strong peak is observed at $3774\,cm^{-1}$ which we assign to a C_2H_5-HF complex. Turning off the electric field we recover the rotationally resolved spectrum shown in figure 10 (A). Figure 10 (C) shows the Stark spectrum for this band recorded at an electric field strength of $3.86\,kV\,cm^{-1}$, from which the dipole moment is derived. The molecular parameters determined from the fits to the spectra are given in table 3, together with the values for the ethyl-HCN complex. In figure 11 (A) and (C) the field-free spectrum and the Stark spectrum of the allyl radical-HF complex are shown, respectively, and the obtained molecular parameters are summarized in table 3, together with the values for the allyl-HCN complex. The results on these larger hydrocarbon radicals are very promising for studying radicals that are even more important in radical chain reactions in combustion processes, such as, for example, $C_nH_{2n+1}OO$ peroxy-radicals, which are some of the most important intermediates in these reactions [196]. High-resolution

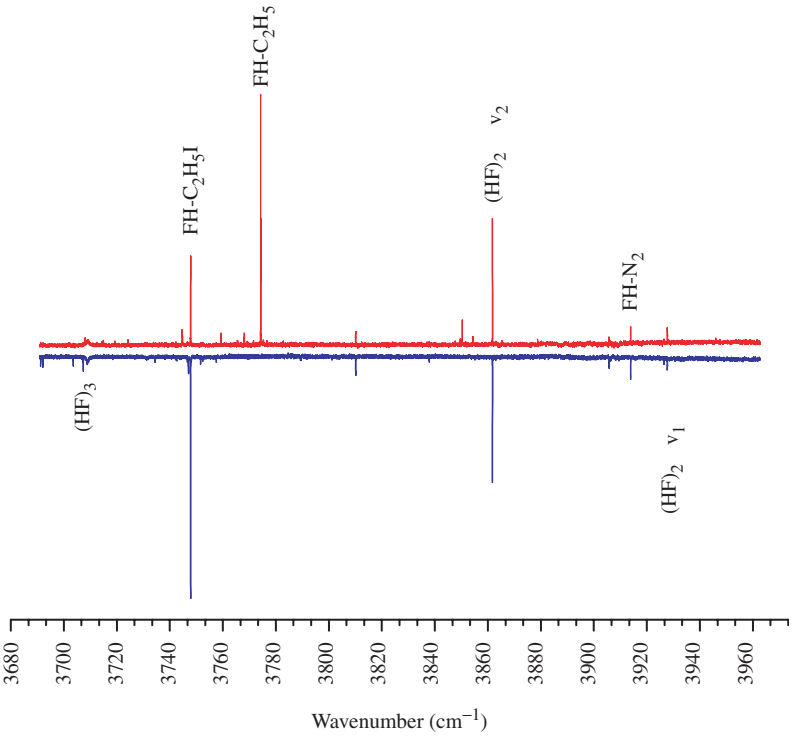

Figure 9. [Colour online] Pendular survey scans corresponding to flowing ethyl iodide through a cold (downward going peaks) or hot (upward going peaks) pyrolysis source. HF is then picked up downstream in a separate pick-up cell. We assign the peak at 3747 cm^{-1} to an HF-C_2H_5I complex, the intensity of which decreases substantially at temperatures appropriate for pyrolysis. At pyrolysis temperatures of about 1000 K, the peak at 3774 cm^{-1} appears which is assigned to the HF-ethyl radical complex.

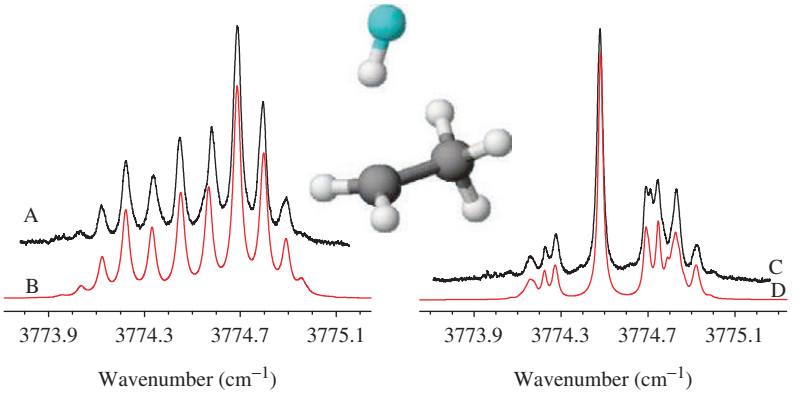

Figure 10. [Colour online] Rotationally resolved field-free (A) and Stark (C) spectra corresponding to the HF stretching vibration of the HF-C_2H_5 complex and the corresponding simulations, (B) and (D), respectively. Inertial parameters and dipole moments are given in table 3.

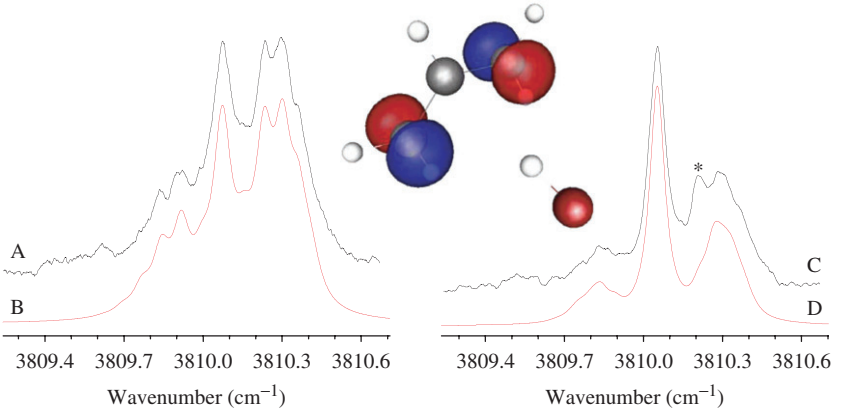

Figure 11. [Colour online] Field-free (A) and Stark (C) spectra for the HF-Allyl radical complex, and the corresponding simulations, (B) and (D), respectively. The peak marked with an asterisk corresponds to a known impurity which overlaps at this frequency. Inertial parameters and dipole moments are given in table 3.

spectra of these molecules have been difficult to obtain in free-jet expansions thus far [197–203].

Moreover, given that we have shown that pure effusive beams of hydrocarbon radicals can be made under suitable conditions for helium droplet pick-up, the possibility of studying radical-radical and radical-molecule reactions inside the helium droplets is reasonable. A very interesting and simple experiment would be to dope a single oxygen molecule into a droplet containing a hydrocarbon radical. Theoretical calculations predict that the reaction to form hydroperoxy radicals (ROO$^{\bullet}$) is barrierless [204], however, at low temperatures this might only apply if the oxygen directly approaches the radical centre. Instead, the helium might trap the complex in a local van der Waals minimum, forming a pre-reactive complex, similar to what is discussed in section 6.1. Vibrational excitation could then be used to initiate the corresponding reaction.

4.3 *NO-HF*

Given the recent observation that the Λ doubling of NO was increased by 55% upon solvation in a helium droplet, there is considerable need to further study this phenomenon, since exciting new molecules and clusters might only be formed in helium, with no gas-phase data available for comparison. This statement is already particularly true given our preliminary results on open-shell clusters with Br, I, Ga, and In atoms which have revealed large parity splittings. Indeed, recent high-level theoretical calculations on the HCN-Br complex indicate that the parity splitting is much smaller in a helium droplet than one might expect in the gas-phase [148]. The electronic angular momentum couplings, which are responsible for such open-shell

Table 4. Molecular constants of the NO-HF complex derived by fitting the experimentally observed spectrum for the HF stretching vibration in both helium droplets and in the gas-phase [205]. The fit to the field-free spectrum was performed using the contour fitting routines in pgopher [206]. Note that in pgopher the signs of p_J must be reversed when compared to the original model of Fawzy [205].

Constant (cm^{-1})	Helium droplet	Gas-phase
ν_0	3871.76	3877.47269(12)
B''	0.0473	0.111320(17)
B'	0.0479	0.116167(19)
p''	0.0676	0.15274(19)
p'	0.0802	0.19652(18)
D''_J	$1.25 \cdot 10^{-4}$	$2.56(31) \cdot 10^{-6}$
D'_J	$1.43 \cdot 10^{-4}$	$2.56(31) \cdot 10^{-6}$
p''_J	$3.8 \cdot 10^{-4}$	$0.932(54) \cdot 10^{-4}$
p'_J	$4.2 \cdot 10^{-4}$	$0.503(38) \cdot 10^{-4}$

effects, are sensitive probes of electronic degrees of freedom. Moreover, there is relatively little information available so far on how the helium droplet effects these couplings. In order to further our understanding of such open-shell species in helium, we have recorded the infrared spectrum of the NO-HF complex, which has been observed previously in the gas-phase by Fawzy *et al.* [205]. Fitting the helium droplet spectrum to the same model Hamiltonian resulted in the molecular constants listed in table 4, which are compared with the gas-phase values [205]. In contrast to NO in helium, we find that for NO-HF, the parity constant p is reduced from the gas-phase value by exactly the same amount (within experimental uncertainty) as the rotational constant B. As pointed out for NO [76], the expression for the parity splitting does have a linear relationship with B, and this is exactly what we see for NO-HF. For NO monomer, however, the parity splitting was increased by 55% despite the fact that the rotational constant was 76% of the gas-phase value, illustrating that the mechanism with which the helium interacts with the molecule is different [76]. The NO-HF results may support the conclusion of von Haeften *et al.* [76], that solvation in the helium droplets result in a symmetry breaking effect due to helium-density fluctuations, resulting in a first order splitting of the two components of the Π state. Due to the fact that NO-HF is a bent complex, with an already reduced symmetry, this symmetry breaking might not be as important as for NO and the decrease in the parity splitting only reflects the change in the effective rotational constant. However, large scale calculations are still needed to test this hypothesis.

5. Interactions between helium droplets and embedded molecules

Since the first spectroscopic investigation of SF_6 embedded in helium droplets in 1992 [207] and the first observation of free rotation thereof a few years later [62], a large number of molecules and cluster systems have been studied and trends are now

being established. The most easily recognized and well publicized trend is the effect of the helium droplet on the associated rotational constants of the embedded cluster. Two dynamical regimes have been established. Light rotors with their large rotational constants do not couple efficiently to the helium, resulting in only a slight decrease in the observed rotational constant compared to the gas phase. In contrast, heavier rotors typically exhibit a much more anisotropic interaction with the helium, which allows some of the helium to follow the rotational motion, thus adding to its moment of inertia. Typically rotational constants of *heavy rotors* ($B < 1\,\mathrm{cm}^{-1}$) are reduced by a factor of 2.5 ± 0.5 when compared to the gas-phase [1]. The scatter in the reduction factors of the rotational constants results from the unique dopant-helium interactions for the individual systems, and, for example, two similar molecules such as CO_2 and N_2O, which have nearly the same gas-phase rotational constant, have very different helium droplet rotational constants due to the differences in the interaction potentials [208]. Since inside helium droplets metastable structures can be formed, which may be impossible to be observed in the gas-phase, there is certainly a desire to be able to extract quantitative bond lengths and angles from the rotationally resolved spectra. Fully quantum mechanical calculations have been able to reproduce the experimentally determined rotational constants for a few prototype systems, which is certainly a first step [209–211]. Despite the ambiguity in rotational constants, the overall symmetry of the system is not affected, which can aid in structural determinations. Indeed the nuclear spin statistical weights for propargyl and all CH_3-HX-type complexes have confirmed the C_{2v} and C_{3v} symmetries of the isolated gas-phase molecules, respectively.

As can be seen from previous reviews on the subject, almost all of our knowledge on the interaction of the droplet with a dopant has come from closed-shell molecules. From the admittedly small group of open-shell molecules studied, which are summarized in this review, we find that the molecule-helium interactions are generally the same for radicals as for closed-shell systems. The biggest exception would be the fact that open-shell alkali and the quasi-closed-shell heavier earth alkali metal atoms are not solvated by the droplets and instead reside on the surface, which generally results from a stronger He-He interaction than the corresponding He-metal interaction. It was first unclear as to whether the interaction with an open-shell molecule would be favourable at all, i.e. whether the radical would go into the droplet, based on the known repulsive interaction between lone electrons and helium droplets [212]. For open-shell atoms in non-S states, i.e. halogen atoms (^2P), the electrostatic interactions with the quadrupole moment of the atom are quite strong, thus in general allowing for solvation.

Even if the species goes into the droplet, a localized unpaired electron may cause density distortions of the surrounding helium, which could lower the overall symmetry. Indeed such effects were postulated for NO [76], which would give rise to a first order splitting of the two parity components. In that light the different effects of the helium droplet environment on the parity splitting of bare NO and the NO-HF complex show how such effects depend on details of the molecular system and the molecule-helium interactions. Theoretical support is urgently needed to describe and understand these detailed experimental results.

6. Future directions

6.1 *High-energy structures for chemical energy storage*

The possibilities to build metastable molecular cluster structures inside liquid helium nanodroplets was demonstrated, for example, by observing a ring of six water molecules [64] or by the self-assembly of long linear chains of HCN [63]. These chains are built up due to the specific kinetic control of the complex formation inside the helium droplets. Since individual molecules are picked up successively by the droplet and are rapidly cooled inside with a rate of $\sim 10^{16}\,\mathrm{K\,s^{-1}}$ [213], they approach each other isothermally at low temperature (0.4 K). Already at relatively long distance polar molecules are oriented in the field produced by the dipole of the complexation partner. The ground state of every polar molecule is high-field seeking and therefore the molecular dipoles of both complexation partners are oriented along the intermolecular axis while they approach each other. Once they are close to each other, they find themselves in a linear, hydrogen bonded geometry. Due to the low temperature they cannot rearrange to form the thermodynamically more stable cyclic structures observed in free jets [214, 215].

In the same way as for HCN it should be possible to assemble chains of polar radicals in helium droplets, e. g. chains of CN or OH radicals. Considering two ground-state OH radicals approaching one another from long range at very low temperatures, the hydrogen peroxide structure is the global minimum product. Nevertheless, theory predicts that there is also a hydrogen bonded minimum at long range analogous to the HF dimer [216, 217]. At long range dipole–dipole interactions dominate and the ground state OH-OH interactions are essentially the same as for the HF dimer. Since the length scale for the hydrogen-bond is very different from that of the chemical well, it is expected that after reaching the hydrogen-bonded well there is a barrier to further bond-compression, before the O–O distance is decreased sufficiently to access the chemical bonding region [218]. In systems with such barriers the possibility exists for stabilizing the pre-reactive complex in the hydrogen bonded well inside a helium droplet, in analogy to the physisorbed state in surface science. The challenge is to remove the condensation energy from the system as it forms, before it can surmount any barriers, thus trapping it in the pre-reactive form. The natural extension to larger OH clusters suggests that one might be able to make a whole new class of pre-reactive radical solids.

The qualitative description given above is supported by extensive theoretical studies of the hydrogen peroxide system [219]. Particularly interesting is a high-level theoretical study by Kuhn *et al.*, in which a minimum energy path analysis shows how the bonding character changes from long range hydrogen bonding to covalent bonding at decreased O–O distances [218]. These two regions are separated by a significant barrier – some hundred wavenumbers for the highest quality potential – that is presumably high enough to exhibit bound states in the hydrogen bonded well. Moreover, the minimum energy path from these calculations shows a cusp at the maximum of the barrier, corresponding to a sudden change in the angular geometry of the complex at that distance. This is due to the need for switching from a

geometry with the molecular dipoles oriented parallel (OH-OH) to an head-to-head structure (HO–OH).

With this theoretical work supporting the existence of a barrier between the hydrogen bonded and the chemical bonded minima, there is good reason to think that the pre-reactive dimer, as well as larger nano-clusters, can be stabilized by following the minimum energy approach path analogous to the production of HCN chains [63], cyclic water hexamer [64], and polymers of HF [220–223]. $(H_2)_n$-HF clusters, which are a good model for the reactive OH/H_2 system, have also been studied in helium droplets [224–227]. These studies show that there is considerable control on the number of molecules picked up by the droplets, allowing the study of a wide range of stoichiometries. It should be emphasized that the $(HCN)_{n\geq 3}$, $(H_2O)_6$, and $(HF)_{n\geq 4}$ systems form different, metastable, structures in liquid helium droplets [63, 64, 223], than obtained from gas-phase nucleation, where typically only the global minimum is observed. The implication is that liquid helium provides a new growth medium for creating and stabilizing higher energy isomers of clusters that are not normally observed in the gas-phase. It is also encouraging that different clusters of quite large size can be differentiated using infrared pendular state spectroscopy [63].

To illustrate what might be achieved by producing analogous metastable structures of radicals, consider the hydrogen–oxygen reactions [228–230]:

$$2H_2 + O_2 \longrightarrow 2H_2O \qquad \Delta_f H^\circ = -484\,\mathrm{kJ\,mol^{-1}}$$
$$H_2 + O_2 \longrightarrow H_2O_2 \qquad \Delta_f H^\circ = -273\,\mathrm{kJ\,mol^{-1}}$$

and for comparison, consider the following reactions:

$$2OH + H_2 \longrightarrow 2H_2O \qquad \Delta_f H^\circ = -562\,\mathrm{kJ\,mol^{-1}}$$
$$2OH \longrightarrow H_2O_2 \qquad \Delta_f H^\circ = -351\,\mathrm{kJ\,mol^{-1}}$$

Thus, if solids of pure OH or with a OH/H_2 ratio of 2 : 1 could be stabilized, these would exhibit exothermicities that are considerably higher than that of the hydrogen–oxygen system, which is widely used as fuel. As such they would be ideal combustibles for high-energy consumptions. From the discussion given above, there is plenty of evidence to suggest this could be achieved, both in nanodroplets and in bulk helium.

Other systems that could potentially provide an even larger amount of chemical energy storage are nitrogen (oxygen) oligomers, which react very exothermally to form stable N_2 (O_2) molecules. The N_3 and N_4 molecules have been predicted [231–233] and observed experimentally [234, 235]. The cluster formation mechanism in helium droplets described above should allow one to produce a wide variety of such metastable N_n systems from nitrogen atoms, where n could be much larger than 3 and is solely determined by the N-atom density in the pick-up region.

Gordon and co-workers [236–239] have shown that similar radical solids can be stabilized in bulk liquid helium.† They directed a helium beam containing atomic

† It was recently proposed that similar effects should also be obtainable in atomic Bose–Einstein condensates, where ionic impurities could lead to the formation of *mesoscopic molecular ions* [240].

nitrogen into a dewar of liquid helium, to find that a highly energetic, snow-like precipitate was formed [236, 238, 239]. Upon warming that material, it thermally detonated. Electron spin measurements have shown an unexpectedly high concentration of N atoms with more than 10% of the N_2 concentration in the original experiments. Later the experiments were optimized to obtain atomic concentrations as high as 50% [237]. Although a number of techniques have been used to study the properties of these cryo-solids, detailed structural information is still lacking. Nevertheless the authors point out that the liquid helium is only necessary during the formation process and have shown that the resulting solids are stable when the liquid helium is completely evaporated, as long as the temperature remains below approximately 8 K [238]. Most remarkably the authors were able to use a plunger to compact the solid precipitate into a pellet without causing it to react [241]. They suggest that the method should be applicable to a wide range of species and we suspect that it will be even more effective for *molecular* radicals, where there are steric considerations that also inhibit recombination. A number of fascinating observations have been made by Gordon and coworkers, including the appearance of an *intense green glow* when the sample was irradiated with an helium neon laser [237, 242]. More recently they showed that captured $N(^2D)$ atoms show thermoluminescence upon slight heating by 0.1 K or when irradiating them using microwaves [243, 244]. Details of the impurity condensation in liquid and solid helium and the interpretation of their X-ray and IR spectroscopic studies have recently been discussed [245].

Structural information on such materials is clearly desirable and can be obtained from vibrational spectroscopy on small (nano-scale) samples of these materials. Studies in liquid helium droplets will provide better control of the growth, as well as the ability to use high-resolution vibrational and rotational spectroscopy to characterize the resulting structures. For smaller clusters rotational resolution will be possible, providing detailed information on the corresponding structures.

The nano-solids we are proposing to make in these studies are highly energetic and it is interesting to consider what will happen when they are vibrationally excited. If the vibrational energy deposited in the molecules is sufficient to overcome the barriers that are responsible for the stability of the clusters, and the energy becomes redistributed into the reaction coordinate by intramolecular vibrational energy redistribution (IVR), it is expected to observe strong responses to the laser excitation. This laser-induced detonation (LID) will result in complete evaporation of the helium droplet resulting in very strong depletion signals. Alternatively, the clusters might dissipate the vibrational energy to the helium so quickly that no reaction occurs and the system simply cools back down by evaporation of helium atoms. These effects could be studied using IR-IR pump-probe experiments, similar to the ones demonstrated for stable species embedded in helium droplets [65, 66]. Considering the OH-OH system, it is interesting to consider excitation of the OH-OH intermolecular vibrations, or excitation of combination modes based on the OH stretching vibration i.e. using combination modes of this vibration. This will put energy into the reaction coordinate and may push the system over the barrier and into the reactive well. Such tests of the stability of these solid materials are important in accessing the usefulness of such materials as specialty fuels. Understanding the growth of such new classes of high-energy density materials in liquid helium can be used to make

and study the properties and structures of these systems on the nanometre scale. What is exciting about this approach is that it has the potential to be scaled up to macroscopic sizes, as demonstrated by the experiments of Gordon and coworkers [236–239, 242, 245].

Considering the Br-HCN and HCN-Br complexes described above, it seems reasonable to allow for the formation of a metastable Br-HCN-Br complex as such a high-energy structure. Whereas we were not able to find this HCN complex, first experiments using the equivalent cyanoacetylene (HCCCN) chromophore suggest the existence of such complexes. In figure 12 pendular survey scans for the bromine-cyanoacetylene system are shown for different experimental conditions. It is important to note that scans 12 (A)–(C) were recorded by picking up the HCCCN first, but in 12 (D) the order has been reversed, and we instead pick-up from the pyrolysis source first. In scan 12 (A), only HCCCN is added to the droplets, while in 12 (B), Br_2 is flowing through a room temperature pyrolysis source. The result of heating the pyrolysis to the appropriate temperatures for bromine atom pick-up are shown in scans 12 (C) and (D). In good agreement with the results of X + HCN, we find two peaks at 3326.1 and 3302.4 cm^{-1}, marked by a †, which we assign to the Br-HCCCN and HCCCN-Br complexes, respectively, based on their frequency shifts and signal strengths. The peaks labelled with an ∗ were found to optimize at higher HCCCN pressure, therefore they correspond to complexes containing more than one HCCCN. The peak at 3297.65 cm^{-1} optimizes at the same HCCCN pressure as the 1 : 1 complexes, however, it is found to optimize at higher bromine pressure,

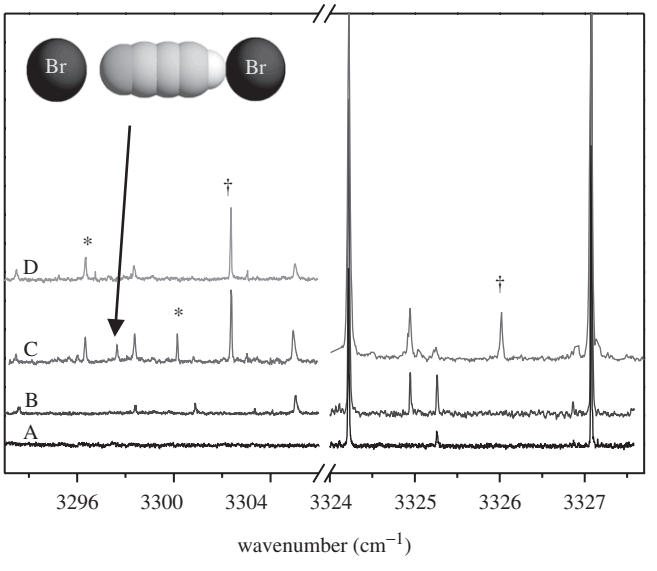

Figure 12. Pendular survey scans for the Br + HCCCN system, where the bromine pressure is intentionally high to facilitate forming larger clusters. In (A) only HCCCN is picked up by the droplets and in (B) Br_2 is flowing through the cold pyrolysis source. Scans (C) and (D) were both recorded with the pyrolysis source at the appropriate temperature for bromine atom production. Whereas in (C) the HCCCN is picked up first, in (D) the bromine atoms are picked up first. See text for details.

suggesting that it is a complex containing two bromine atoms [132, 170]. Since it only appears in the spectrum when the HCCCN is picked up first, it is a good candidate for being Br-HCCCN-Br, a metastable van der Waals complex containing two spatially separated bromine atoms. The dependence on pick-up order is to be expected because two bromine atoms will likely recombine to form Br_2 in the absence of the molecular spacer.

To aid in this preliminary assignment we performed bromine pressure dependence measurements [132]. This new peak is found to optimize at higher bromine pressures than those peaks assigned to the 1 : 1 complexes, and agrees well with a simulation of a dimer using a Poisson distribution for the pick-up statistics. Although we cannot rule out that a Br-HCCCN-Br_2, or similar complex might have such a pick-up cell pressure dependence, a double-resonance population transfer experiment [66] in which this new peak is pumped and the HCCCN-Br_2 complex is recovered would be definitive.

It is also interesting to note, that the original interest in stabilizing spin-polarized hydrogen arose because of the same reasons, namely searching for novel high-energy structures [246–248]. The reaction $H + H \rightarrow H_2$ is exothermic by more than $400\,kJ\,mol^{-1}$, yielding a very large energy-to-mass ratio if samples of atomic hydrogen could be stabilized. For two polarized hydrogen atoms direct molecule formation is not possible, as their $^3\Sigma_u^+$ potential is purely repulsive, and a spin-flip is necessary for the binding energy of the hydrogen molecule to be released. Whereas the preparation of dense samples of spin-polarized hydrogen for energy storage has not been successful yet, these studies emerged into the quest for the experimental realization of Bose–Einstein condensation and yielded a whole new field in atomic and molecular physics [249, 250]. Nowadays similar ideas are also discussed in the context of deep space propulsion systems based on antihydrogen [251].

6.2 *Other applications*

Recently a new experiment for a sensitive search for the electric dipole moment (EDM) of the electron using matrix-isolated dipolar radicals was proposed [252]. It was suggested that one should measure the magnetization of an oriented sample of diatomic radicals embedded in a solid noble-gas matrix. While the solid state matrix will provide a larger number density of radicals, it is not clear to what degree molecular orientation can be achieved, since neither the break-down voltages of the matrix nor the details of the cage effects in the matrix sites are known [252]. As shown for several examples in this review, pendular states with a high degree of orientation can easily be achieved for polar molecules embedded in liquid helium droplets. Therefore, the techniques of strong field orientation of radicals embedded in liquid helium droplets, as described in this review, might provide a well-defined environment for sensitive EDM tests.

The OH radical receives considerable attention also in the field of ultracold polar molecules and it has been successfully confined in electrostatic traps for times $> 1\,s$ and at temperatures of $\sim 50\,mK$ [27, 253], and there is considerable interest in cooling such trapped molecules to even lower temperatures. In that context the interaction of two OH molecules at very long range has been considered and for two rotational

ground state OH radicals in their low-field seeking state, so-called *field-linked* states have been predicted: bound states of long-range OH-OH dipole-aligned dimers that are stabilized by an external electric field of the order of $10\,\mathrm{kV\,cm^{-1}}$ [254]. Such field linked states provide a similar degree of control over the chemical reaction as the van der Waals-dimers described above. As long as the field is on, they are safely separated by several nanometres in their long-range well, but when the field is ramped down they can react – assuming that, for example, the exothermic reaction $2\,OH \rightarrow H_2O + O$ proceeds at ultracold temperatures [254]. However, a gas of OH radicals in low-field seeking states is subject to large collisional losses and is therefore not suitable for evaporative cooling [255]. The high-field seeking state is collisionally stable, being the lowest energy state of OH, however, it does not show such long-range states and the collisional parameters are strongly depending on the short-range potential and must be determined by a 'suitable experiment' [254]. Experiments on entrance-channel complexes in helium droplets, like the ones described in this paper, would provide detailed information on this PES.†

6.3 *Experimental improvements*

The main hurdle for studying transient species embedded in superfluid helium droplets is the generation of the necessary clean samples of radicals. Albeit the continuous pyrolysis source [70] proves to be a very successful and versatile tool for the production of a wide range of radicals, the types of radicals that can be produced is still quite limited. It seems impossible, for example, to use it to create clean sources of oxygen or nitrogen atoms, as necessary for the experiments proposed above, as that would require to thermally break the extremely strong O_2 or N_2 bonds.

Alternative techniques that have been used so successfully in free jet experiments, such as photolysis or discharge sources, cannot easily be coupled to typical droplet beam setups, which in the vast majority are operated in a cw fashion. Once pulsed droplet beams mature [88, 89] they will provide much larger droplet densities, which might allow to couple them to pulsed radical sources. Nevertheless, the droplet property of embedding any species in the scattering region requires extremely clean sources that would still need to be developed, but the possibility of using photodissociation should help considerably to break strong bonds.

It would be extremely interesting to perform time-resolved studies on the processes of molecules embedded in helium droplets in order to study reactions and relaxation dynamics in real time. Femtosecond pump-probe experiments on alkali-doped helium droplets [257–259] show the feasibility of such experiments. In these experiments the dynamics of the helium-alkali atom interaction could be clearly observed. In a similar way it should be possible to observe relaxation dynamics after vibrational excitation of molecules like HCN embedded *inside* the helium droplets. Once metastable radical complexes, as described above, can be produced inside the helium droplets one could

† In a similar approach groups from the field of ultracold atomic physics and helium droplet spectroscopy have successfully collaborated to obtain information on the PES and spectroscopy of mixed alkali dimers [256].

even photoinitiate their reaction and follow the complete chemical dynamics from the reactants to the final products due to the confining environment of the droplets.

7. Summary

Superfluid helium droplets provide a novel medium for the study of transient and reactive species. A continuous pyrolysis source for the production of extremely clean, effusive beams of radicals suitable for pick-up by helium droplet beams has been developed and the radicals embedded in helium droplets have been studied using high-resolution infrared spectroscopy. Using this setup, halogen atoms and hydrocarbon radicals have been produced and their van der Waals complexes with HF or HCN examined. In related studies NO and also a few other transient molecules have been studied as well. Many of the systems investigated provide new, detailed information on stationary points of PES that were previously only studied using reactive scattering experiments. Even further information and the possibility for optically controlled chemistry can be obtained using double-resonance techniques.

The results from these studies also provide a very sensitive probe of the quantum fluid nature of the helium droplet. The droplet not only influences the inertial parameters, as for closed-shell molecules, but also the electronic properties, such as parity splittings and Λ-doubling parameters.

The ability to design complexes of multiple, potentially different stable and transient species inside these cryo-reactors promises a wide variety of possibilities: studying stationary points on the PES of these reactive species; developing novel high-energy species; studying reaction dynamics under cold and defined conditions; and studying optically induced chemical reactions.

The extraction of quantitative structural data from high-resolution spectra of molecules embedded in helium droplets is still quite limited, due to the lack of accurate models for the molecule-helium droplet interaction. However, progress in the theoretical descriptions of these effects might allow one to determine accurate structural information, i.e. geometric rotational constants, for the isolated molecular systems from helium droplet experiments.

Acknowledgments

Most of the experimental work described herein was performed at the University of North Carolina at Chapel Hill in the group of Roger Miller, who died on 6 November 2005. The authors are very grateful for the opportunity to work with him and for the stimulating environment and support he provided to his group.

J. M. M. thanks Tom Baer for supporting him during the final stage of his graduate work. We thank Ad van der Avoird for providing the potential energy surfaces in figure 3. We wish to acknowledge detailed feedback by one referee.

Financial support by NSF and AFOSR is acknowledged. J. K. gratefully acknowledges a Feodor Lynen fellowship of the Alexander von Humboldt Foundation and J. M. M. a scholarship by the Max Planck Society.

References

[1] M. Y. Choi, G. E. Douberly, T. M. Falconer, W. K. Lewis, C. M. Lindsay, J. M. Merritt, P. L. Stiles, and R. E. Miller, Int. Rev. Phys. Chem. **25,** 15 (2006).
[2] F. Stienkemeier and K. K. Lehmann, J. Phys. B **39,** R127 (2006).
[3] J. P. Toennies and A. F. Vilesov, Angew. Chem. Int. Ed. **43,** 2622 (2004).
[4] G. N. Makarov, Physics-Uspekhi **47,** 217 (2004).
[5] J. A. Northby, J. Chem. Phys. **115,** 10065 (2001).
[6] C. Callegari, K. K. Lehmann, R. Schmied, and G. Scoles, J. Chem. Phys. **115,** 10090 (2001).
[7] F. Stienkemeier and A. F. Vilesov, J. Chem. Phys. **115,** 10119 (2001).
[8] J. Warnatz, U. Maas, and W. Dibble, *Combustion: Physical and Chemical Fundamentals, Modeling and Simulation, Experiments: Pollutant Formation* (Springer, Berlin, 1996).
[9] R. P. Wayne, *Chemistry of Atmospheres: An introduction to the Chemistry of the Atmospheres of Earth, the Planets, and their satellites* (Oxford University Press, Oxford, 1991), 2nd edn.
[10] D. Chastaing, P. L. James, I. R. Sims, and I. W. M. Smith, Phys. Chem. Chem. Phys. **1,** 2247 (1999).
[11] J. H. Van't Hoff, *Études de dynamique chimique* (Muller, Amsterdam, 1884).
[12] S. Arrhenius, Z. Phys. Chem. **4,** 226 (1889).
[13] F. London, Z. Phys. Chem. **35,** 552 (1929).
[14] H. Eyring and M. Polanyi, Z. Phys. Chem. B **12,** 279 (1931).
[15] G. S. Hammond, J. Am. Chem. Soc. **77,** 334 (1955).
[16] J. C. Polanyi and W. H. Wong, J. Chem. Phys. **51,** 1439 (1969).
[17] J. J. Valentini, Ann. Rev. Phys. Chem. **52,** 15 (2001).
[18] S. D. Chao, S. A. Harich, D. X. Dai, C. C. Wang, X. M. Yang, and R. T. Skodje, J. Chem. Phys. **117,** 8341 (2002).
[19] M. H. Qiu, Z. F. Ren, L. Che, D. X. Dai, S. A. Harich, X. Y. Wang, X. M. Yang, C. X. Xu, D. Q. Xie, M. Gustafsson, R. T. Skodje, Z. G. Sun, and D. H. Zhang, Science **311,** 1440 (2006).
[20] J. Y. Zhang, D. X. Dai, C. C. Wang, S. A. Harich, X. Y. Wang, X. M. Yang, M. Gustafsson, and R. T. Skodje, Phys. Rev. Lett. **96,** 093201 (2006).
[21] D. H. Parker and R. B. Bernstein, Ann. Rev. Phys. Chem. **40,** 561 (1989).
[22] H. J. Loesch, Ann. Rev. Phys. Chem. **46,** 555 (1995).
[23] A. J. OrrEwing, J. Chem. Soc. – Faraday Trans. **92,** 881 (1996).
[24] P. Casavecchia, Rep. Prog. Phys. **63,** 355 (2000).
[25] H. L. Bethlem, G. Berden, and G. Meijer, Phys. Rev. Lett. **83,** 1558 (1999).
[26] H. L. Bethlem and G. Meijer, Int. Rev. Phys. Chem. **22,** 73 (2003).
[27] S. Y. T. van de Meerakker, N. Vanhaecke, and G. Meijer, Ann. Rev. Phys. Chem. **57,** 159 (2006).
[28] C. E. Heiner, H. L. Bethlem, and G. Meijer, Phys. Chem. Chem. Phys. **8,** 2666 (2006).
[29] H. L. Bethlem, M. R. Tarbutt, J. Küpper, D. Carty, K. Wohlfart, E. A. Hinds, and G. Meijer, J. Phys. B **39,** R263 (2006).
[30] J. J. Gilijamse, S. Hoekstra, S. Y. T. van de Meerakker, G. C. Groeneboom, and G. Meijer, Science **313,** 1617 (2006).
[31] P. F. Weck and N. Balakrishnan, Int. Rev. Phys. Chem. **25,** 283 (2006).
[32] H. J. Werner, W. Bian, M. Menendez, F. J. Aoiz, P. Casavecchia, L. Cartechini, and N. Balucani, Chem. Phys. Lett. **328,** 500 (2000).
[33] H. J. Werner, W. Bian, and U. Manthe, Chem. Phys. Lett. **313,** 647 (1999).
[34] D. Skouteris, D. E. Manolopoulos, W. Bian, H. J. Werner, L. H. Lai, and K. Liu, Science **286,** 1713 (1999).
[35] N. Balakrishnan, J. Chem. Phys. **121,** 5563 (2004).
[36] D. Townsend, S. A. Lahankar, S. K. Lee, S. D. Chambreau, A. G. Suits, X. Zhang, J. Rheinecker, L. B. Harding, and J. M. Bowman, Science **306,** 1158 (2004).
[37] S. D. Chambreau, D. Townsend, S. A. Lahankar, S. K. Lee, and A. G. Suits, Physica Scripta **73,** C89 (2006).
[38] C. Murray and A. J. Orr-Ewing, Int. Rev. Phys. Chem. **23,** 435 (2004).
[39] Y. Kim and H. Meyer, Int. Rev. Phys. Chem. **20,** 219 (2001).
[40] M. C. Heaven, Int. Rev. Phys. Chem. **24,** 375 (2005).
[41] M. I. Lester, B. V. Pond, M. D. Marshall, D. T. Anderson, L. B. Harding, and A. F. Wagner, Faraday Disc. **118,** 373 (2001).
[42] R. A. Loomis, R. L. Schwartz, and M. I. Lester, J. Chem. Phys. **104,** 6984 (1996).
[43] D. T. Anderson, R. L. Schwartz, M. W. Todd, and M. I. Lester, J. Chem. Phys. **109,** 3461 (1998).
[44] R. A. Loomis and M. I. Lester, Ann. Rev. Phys. Chem. **48,** 643 (1997).

[45] R. L. Schwartz, D. T. Anderson, M. W. Todd, and M. I. Lester, Chem. Phys. Lett. **273,** 18 (1997).
[46] J. M. Hossenlopp, D. T. Anderson, M. W. Todd, and M. I. Lester, J. Chem. Phys. **109,** 10707 (1998).
[47] Y. L. Chen and M. C. Heaven, J. Chem. Phys. **109,** 5171 (1998).
[48] A. L. Kaledin and M. C. Heaven, Chem. Phys. Lett. **347,** 199 (2001).
[49] Y. L. Chen and M. C. Heaven, J. Chem. Phys. **112,** 7416 (2000).
[50] M. D. Wheeler, D. T. Anderson, and M. I. Lester, Int. Rev. Phys. Chem. **19,** 501 (2000).
[51] A. F. Wagner and R. A. Bair, Int. J. Chem. Kinet. **18,** 473 (1986).
[52] G. Ochoa de Aspuru and D. Clary, J. Phys. Chem. A **102,** 9631 (1998).
[53] G. Wu, G. C. Schatz, G. Lendvay, D.-C. Fang, and L. B. Harding, J. Chem. Phys. **113,** 3150 (2000).
[54] M. E. Jacox, Chem. Phys. **42,** 133 (1979).
[55] Z. Mielke and L. Andrews, J. Phys. Chem. **94,** 3519 (1990).
[56] L. Khriachtchev, H. Tanskanen, and M. Rasanen, J. Chem. Phys. **124,** 181101 (2006).
[57] T. Momose, H. Hoshina, M. Fushitani, and H. Katsuki, Vib. Spectrosc. **34,** 95 (2004).
[58] T. Momose, M. Fushitani, and H. Hoshina, Int. Rev. Phys. Chem. **24,** 533 (2005).
[59] K. Yoshioka, P. L. Raston, and D. T. Anderson, Int. Rev. Phys. Chem. **25,** 469 (2006).
[60] T. Momose, H. Hoshina, N. Sogoshi, H. Katsuki, T. Wakabayashi, and T. Shida, J. Chem. Phys. **108,** 7334 (1998).
[61] S. Grebenev, J. P. Toennies, and A. F. Vilesov, Science **279,** 2083 (1998).
[62] M. Hartmann, R. E. Miller, J. P. Toennies, and A. F. Vilesov, Phys. Rev. Lett. **75,** 1566 (1995).
[63] K. Nauta and R. E. Miller, Science **283,** 1895 (1999).
[64] K. Nauta and R. E. Miller, Science **287,** 293 (2000).
[65] J. M. Merritt, G. E. Douberly, and R. E. Miller, J. Chem. Phys. **121,** 1309 (2004).
[66] G. E. Douberly, J. M. Merritt, and R. E. Miller, Phys. Chem. Chem. Phys. **7,** 463 (2005).
[67] D. M. Brink and S. Stringari, Z. Phys. D **15,** 257 (1990).
[68] F. Dalfovo and S. Stringari, J. Chem. Phys. **115,** 1078 (2001).
[69] K. K. Lehmann, J. Chem. Phys. **119,** 3336 (2003).
[70] J. Küpper, J. M. Merritt, and R. E. Miller, J. Chem. Phys. **117,** 647 (2002).
[71] P. A. Block, E. J. Bohac, and R. E. Miller, Phys. Rev. Lett. **68,** 1303 (1992).
[72] E. W. Becker, R. Klingelhofer, and P. Lohse, Z. Naturforsch. A **16,** 1259 (1961).
[73] K. Nauta and R. E. Miller, J. Chem. Phys. **115,** 10138 (2001).
[74] K. Nauta and R. E. Miller, J. Chem. Phys. **113,** 9466 (2000).
[75] C. M. Lindsay, W. K. Lewis, and R. E. Miller, J. Chem. Phys. **121,** 6095 (2004).
[76] K. von Haeften, A. Metzelthin, S. Rudolph, V. Staemmler, and M. Havenith, Phys. Rev. Lett. **95,** 215301 (2005).
[77] H. Pauly, in [260], Chap. 4, pp. 83–123.
[78] H. Pauly, in [260], Chap. 5, pp. 124–152.
[79] D. W. Kohn, H. Clauberg, and P. Chen, Rev. Sci. Instrum. **63,** 4003 (1992).
[80] M. R. Cameron and S. H. Kable, Rev. Sci. Instrum. **67,** 283 (1996).
[81] X. Zhang, A. V. Friderichsen, S. Nandi, G. B. Ellison, D. E. David, J. T. McKinnon, T. G. Lindeman, D. C. Dayton, and M. R. Nimlos, Rev. Sci. Instrum. **74,** 3077 (2003).
[82] P. C. Engelking, Rev. Sci. Instrum. **57,** 2274 (1986).
[83] P. C. Engelking, Chem. Rev. **91,** 399 (1991).
[84] D. T. Anderson, S. Davis, T. S. Zwier, and D. J. Nesbitt, Chem. Phys. Lett. **258,** 207 (1996).
[85] D. L. Monts, T. G. Dietz, M. A. Duncan, and R. E. Smalley, Chem. Phys. **45,** 133 (1980).
[86] M. Heaven, T. A. Miller, and V. E. Bondybey, Chem. Phys. Lett. **84,** 1 (1981).
[87] P. Andresen, D. Häusler, and H. W. Lülf, J. Chem. Phys. **81,** 571 (1984).
[88] M. N. Slipchenko, S. Kuma, T. Momose, and A. F. Vilesov, Rev. Sci. Instrum. **73,** 3600 (2002).
[89] S. Yang, S. M. Brereton, and A. M. Ellis, Rev. Sci. Instrum. **76,** 104102 (2005).
[90] K. Lehmann, Faraday Disc. **118,** 55 (2001), in general discussion.
[91] A. Conjusteau, Ph.D. thesis, Princeton University, Princeton, NJ, USA (2002).
[92] D. Stolyarov, E. Polyakova, and C. Wittig, J. Phys. Chem. A **108,** 9841 (2004).
[93] A. Braun and M. Drabbels, Phys. Rev. Lett. **93,** 253401 (2004).
[94] K. Kavita and P. K. Das, J. Chem. Phys. **112,** 8426 (2000).
[95] D. H. Parker and A. Eppink, J. Chem. Phys. **107,** 2357 (1997).
[96] M. Fárník and J. P. Toennies, J. Chem. Phys. **122,** 014307 (2005).
[97] W. K. Lewis, C. M. Lindsay, R. J. Bemish, and R. E. Miller, J. Am. Chem. Soc. **127,** 7235 (2005).
[98] N. M. Marinov, W. J. Pitz, C. K. Westbrook, A. M. Vincitore, M. J. Castaldi, S. M. Senkan, and C. F. Melius, Combust. Flame **114,** 192 (1998).
[99] P. R. Westmoreland, A. M. Dean, J. B. Howard, and J. P. Longwell, J. Phys. Chem. **93,** 8171 (1989).
[100] U. Alkemade and K. H. Homann, Z. Phys. Chem. **161,** 19 (1989).

[101] S. E. Stein, J. A. Walker, M. M. Suryan, and A. Fahr, in *Symp. (Int.) Combust*. (1990), vol. 23, pp. 85–90.
[102] P. Botschwina, R. Oswald, J. Flügge, and M. Horn, Z. Phys. Chem. **188,** 29 (1995).
[103] P. Botschwina, M. Horn, R. Oswald, and S. Schmatz, J. Electron. Spectrosc. **108,** 109 (2000).
[104] H. Honjou, M. Yoshimine, and J. Pacansky, J. Phys. Chem. **91,** 4455 (1987).
[105] A. Hinchcliffe, J. Mol. Struct. **37,** 295 (1977).
[106] C. H. Wu and R. D. Kern, J. Phys. Chem. **91,** 6291 (1987).
[107] N. M. Marinov, M. J. Castaldi, C. F. Melius, and W. Tsang, Combust. Sci. Technol. **128,** 295 (1997).
[108] I. Glassman, in *Symp. (Int.) Combust*. (1988), vol. 22, p. 295.
[109] J. A. Miller, in *Symp. (Int.) Combust*. (1996), vol. 26, p. 461.
[110] J. M. Goodings, D. K. Bohme, and C.-W. Ng, Combust. Flame **36,** 27 (1979).
[111] D. B. Olson and H. F. Calcote, in *Symp. (Int.) Combust*. (1981), vol. 18, p. 453.
[112] K. Tanaka, T. Harada, K. Sakaguchi, K. Harada, and T. Tanaka, J. Chem. Phys. **103,** 6450 (1995).
[113] L. Yuan, J. DeSain, and R. F. Curl, J. Mol. Spec. **187,** 102 (1998).
[114] K. Tanaka, Y. Sumiyoshi, Y. Ohshima, Y. Endo, and K. Kawaguchi, J. Chem. Phys. **107,** 2728 (1997).
[115] P. L. Chapovsky and L. J. F. Hermans, Ann. Rev. Phys. Chem. **50,** 315 (1999).
[116] M. Fushitani and T. Momose, J. Chem. Phys. **116,** 10739 (2002).
[117] P. L. Stiles, K. Nauta, and R. E. Miller, Phys. Rev. Lett. **90,** 135301 (2003).
[118] P. Botschwina, *The zero-point corrected dipole moment of propargyl radical* private communication (2002).
[119] E. Polyakova, D. Stolyarov, and C. Wittig, J. Chem. Phys. **124,** 214308 (2006).
[120] L. Meyer and F. Reif, Phys. Rev. **110,** 279 (1958).
[121] K. R. Atkins, Phys. Rev. **116,** 1339 (1959).
[122] W. W. Johnson and W. I. Glaberson, Phys. Rev. Lett. **29,** 214 (1972).
[123] K. K. Lehmann and J. A. Northby, Mol. Phys. **97,** 639 (1999).
[124] F. Stienkemeier, J. Higgins, W. E. Ernst, and G. Scoles, Z. Phys. B **98,** 413 (1995).
[125] J. Reho, C. Callegari, J. Higgins, W. E. Ernst, K. K. Lehmann, and G. Scoles, Faraday Disc. **108,** 161 (1997).
[126] F. R. Brühl, R. A. Trasca, and W. E. Ernst, J. Chem. Phys. **115,** 10220 (2001).
[127] E. Lugovoj, J. P. Toennies, and A. Vilesov, J. Chem. Phys. **112,** 8217 (2000).
[128] E. Herbst and W. Klemperer, Astron. J. **185,** 505 (1973).
[129] D. Smith, Chem. Rev. **92,** 1473 (1992).
[130] D. M. Neumark, Phys. Chem. Comm **5,** 76 (2002).
[131] A. J. C. Varandas, P. J. S. B. Caridade, J. Z. H. Zhang, Q. Cui, and K. L. Han, J. Chem. Phys. **125,** 064312 (2006).
[132] J. M. Merritt, J. Küpper, and R. E. Miller, Phys. Chem. Chem. Phys. **9**, 401 (2007).
[133] J. M. Merritt, J. Küpper, and R. E. Miller, Phys. Chem. Chem. Phys. **7,** 67 (2005).
[134] M.-L. Dubernet and J. M. Hutson, J. Chem. Phys. **101,** 1939 (1994).
[135] M.-L. Dubernet and J. M. Hutson, J. Phys. Chem. **98,** 5844 (1994).
[136] C. S. Maierle, G. C. Schatz, M. S. Gordon, P. Mccabe, and J. N. Connor, J. Chem. Soc. – Faraday Trans. **93,** 709 (1997).
[137] P. Jungwirth, P. Zdanska, and B. Schmidt, J. Phys. Chem. A **102,** 7241 (1998).
[138] M. Bittererova and S. Biskupic, Chem. Phys. Lett. **299,** 145 (1999).
[139] M. Meuwly and J. M. Hutson, Phys. Chem. Chem. Phys. **2,** 441 (2000).
[140] M. Meuwly and J. M. Hutson, J. Chem. Phys. **112,** 592 (2000).
[141] M. Meuwly and J. M. Hutson, J. Chem. Phys. **119,** 8873 (2003).
[142] J. A. Kłos, G. Chałasiński, M. M. Szczęśniak, and H.-J. Werner, J. Chem. Phys. **115,** 3085 (2001).
[143] W. B. Zeimen, J. A. Kłos, G. C. Groenenboom, and A. van der Avoird, J. Phys. Chem. A **107,** 5110 (2003), see erratum: [261].
[144] D. M. Neumark, Ann. Rev. Phys. Chem. **43,** 153 (1992).
[145] M. P. Deskevich, M. Y. Hayes, K. Takahashi, R. T. Skodje, and D. J. Nesbitt, J. Chem. Phys. **124,** 224303 (2006).
[146] A. V. Fishchuk, P. E. S. Wormer, and A. van der Avoird, J. Phys. Chem. A **110,** 5273 (2006).
[147] A. V. Fishchuk, G. C. Groenenboom, and A. van der Avoird, J. Phys. Chem. A **110,** 5280 (2006).
[148] A. V. Fishchuk, J. M. Merritt, and A. van der Avoird, submitted to J. Phys. Chem. A; A. V. Fishchuk, J. M. Merritt, G. C. Groenenboom, and A. van der Avoird, submitted to J. Phys. Chem. A.
[149] K. Liu, A. Kolessov, J. W. Partin, I. Bezel, and C. Wittig, Chem. Phys. Lett. **299,** 374 (1999).
[150] K. Imura, H. Ohoyama, R. Naaman, D. C. Che, M. Hashinokuchi, and T. Kasai, J. Mol. Struct. **552,** 137 (2000).
[151] J. M. Mestdagh, B. Soep, M. A. Gaveau, and J. P. Visticot, Int. Rev. Phys. Chem. **22,** 285 (2003).
[152] L. Andrews and R. D. Hunt, J. Chem. Phys. **89,** 3502 (1988).

[153] R. D. Hunt and L. Andrews, J. Chem. Phys. **88,** 3599 (1988).
[154] R. D. Hunt and L. Andrews, J. Phys. Chem. **92,** 3769 (1988).
[155] A. M. G. Ding, L. J. Kirsch, D. S. Perry, J. C. Polanyi, and J. L. Schreiber, Faraday Disc. Chem. Soc. **55,** 252 (1973).
[156] E. Würzberg, A. J. Grimley, and P. L. Houston, Chem. Phys. Lett. **57,** 373 (1978).
[157] E. Würzberg and P. L. Houston, J. Chem. Phys. **72,** 5915 (1980).
[158] C. M. Moore, I. W. M. Smith, and D. W. A. Stewart, Int. J. Chem. Kin. **26,** 813 (1994).
[159] K. Tamagake, D. W. Setser, and J. P. Sung, J. Chem. Phys. **73,** 2203 (1980).
[160] A. Zolot and D. J. Nesbitt, manuscript in preparation.
[161] R. B. Metz, J. M. Pfeiffer, J. D. Thoemke, and F. F. Crim, Chem. Phys. Lett. **221,** 347 (1994).
[162] C. Kreher, R. Theinl, and K. H. Gericke, J. Chem. Phys. **104,** 4481 (1996).
[163] B. K. Decker, G. He, I. Tokue, and R. G. Macdonald, J. Phys. Chem. A **105,** 5759 (2001).
[164] M. Y. Hayes, M. P. Deskevich, D. J. Nesbitt, K. Takahashi, and R. T. Skodje, J. Phys. Chem. A **110,** 436 (2006).
[165] O. D. Krogh and G. C. Pimentel, J. Chem. Phys. **67,** 2993 (1977).
[166] J. O. Hirschfelder, C. F. Curtiss, and R. B. Bird, *Molecular Theory of Gases and Liquids*, vol. 2 (John Wiley, New York, 1965).
[167] A. J. Stone, *The Theory of Intermolecular Forces* (Oxford University Press, Oxford, 1996).
[168] H. J. Loesch and A. Remscheid, J. Chem. Phys. **93,** 4779 (1990).
[169] J. M. Rost, J. C. Griffin, B. Friedrich, and D. R. Herschbach, Phys. Rev. Lett. **68,** 1299 (1992).
[170] J. M. Merritt, Ph.D. thesis, University of North Carolina at Chapel Hill, Chapel Hill, NC, USA (2006).
[171] R. D. Hunt and L. Andrews, Inorg. Chem. **26,** 3051 (1987).
[172] I. U. Goldschleger, A. V. Akimov, E. Y. Misochko, and C. A. Wight, Mendeleev Comm. pp. 43–45 (2001).
[173] K. Schneider, P. Kramper, S. Schiller, and J. Mlynek, Opt. Lett. **22,** 1293 (1997).
[174] M. van Herpen, S. te Lintel Hekkert, S. E. Bisson, and F. J. M. Harren, Opt. Lett. **27,** 640 (2002).
[175] J. M. Merritt and R. E. Miller, in preparation.
[176] G. E. Douberly, P. L. Stiles, and R. E. Miller, to be published.
[177] G. E. Douberly, Ph.D. thesis, University of North Carolina at Chapel Hill, Chapel Hill, NC, USA (2006).
[178] P. L. Stiles and R. E. Miller, J. Phys. Chem. A **110,** 5620 (2006).
[179] K. Nauta, D. T. Moore, P. L. Stiles, and R. E. Miller, Science **292,** 481 (2001).
[180] P. L. Stiles, D. T. Moore, and R. E. Miller, J. Chem. Phys. **121,** 3130 (2004).
[181] D. T. Moore and R. E. Miller, J. Phys. Chem. A **108,** 9908 (2004).
[182] F. Dong and R. E. Miller, J. Phys. Chem. A **108,** 2181 (2004).
[183] W. Shiu, J. J. Lin, and K. Liu, Phys. Rev. Lett. **92,** 103201 (2004).
[184] T. S. Chu, X. Zhang, L. P. Ju, L. Yao, K. L. Han, M. L. Wang, and J. Z. H. Zhang, Chem. Phys. Lett. **424,** 243 (2006).
[185] G. L. Johnson and L. Andrews, J. Am. Chem. Soc. **102,** 5736 (1980).
[186] E. Y. Misochko, V. A. Benderskii, A. U. Goldschleger, A. V. Akimov, and A. F. Shestakov, J. Am. Chem. Soc. **117,** 11997 (1995).
[187] E. Y. Misochko, V. A. Benderskii, A. U. Goldschleger, A. V. Akimov, A. V. Benderskii, and C. A. Wight, J. Chem. Phys. **106,** 3146 (1996).
[188] J. M. Merritt, S. Rudić, and R. E. Miller, J. Chem. Phys. **124,** 084301 (2006).
[189] S. Rudić, J. M. Merritt, and R. E. Miller, J. Chem. Phys. **124,** 104305 (2006).
[190] T. J. Sears, J. M. Frye, V. Spirko, and W. P. Kraemer, J. Chem. Phys. **90,** 2125 (1989).
[191] Z. Liu, H. Gomez, and D. M. Neumark, Chem. Phys. Lett. **332,** 65 (2000).
[192] K. P. Liu, Ann. Rev. Phys. Chem. **52,** 139 (2001).
[193] T. Gilbert, T. L. Grebner, I. Fischer, and P. Chen, J. Chem. Phys. **110,** 5485 (1999).
[194] L. Castiglioni, A. Bach, and P. Chen, J. Phys. Chem. A **109,** 962 (2005).
[195] S. J. Blanksby and G. B. Ellison, Acct. Chem. Res. **36,** 255 (2003).
[196] H. J. Curran, P. Gaffuri, W. J. Pitz, and C. K. Westbrook, Combust. Flame **114,** 149 (1998).
[197] O. J. Nielsen and T. J. Wallington, *Ultraviolet Absorption Spectra of Peroxy Radicals in the Gas Phase* (John Wiley, New York, 1997), pp. 72–73.
[198] M. B. Pushkarsky, S. J. Zalyubovsky, and T. A. Miller, J. Chem. Phys. **112,** 10695 (2000).
[199] S. J. Zalyubovsky, B. G. Glover, and T. A. Miller, J. Phys. Chem. A **107,** 7704 (2003).
[200] S. J. Zalyubovsky, B. G. Glover, T. A. Miller, C. Hayes, J. K. Merle, and C. M. Hadad, J. Phys. Chem. A **109,** 1308 (2005).
[201] B. G. Glover and T. A. Miller, J. Phys. Chem. A **109,** 11191 (2005).
[202] G. Tarczay, S. J. Zalyubovsky, and T. A. Miller, Chem. Phys. Lett. **406,** 81 (2005).
[203] T. A. Miller, Molecular Physics **104,** 2581 (2006).

[204] J. C. Rienstra-Kiracofe, W. D. Allen, and H. F. Schaefer, III, J. Phys. Chem. A **104,** 9823 (2000).
[205] W. M. Fawzy, G. T. Fraser, J. T. Hougen, and A. S. Pine, J. Chem. Phys. **93,** 2992 (1990).
[206] C. M. Western, *Pgopher, a program for simulating rotational structure*, University of Bristol, Bristol.
[207] S. Goyal, D. L. Schutt, and G. Scoles, Phys. Rev. Lett. **69,** 933 (1992), see erratum [262].
[208] K. Nauta and R. E. Miller, J. Chem. Phys. **115,** 10254 (2001).
[209] E. Lee, D. Farrelly, and K. B. Whaley, Phys. Rev. Lett. **83,** 3812 (1999).
[210] A. Viel and K. B. Whaley, J. Chem. Phys. **115,** 10186 (2001).
[211] N. Blinov, X. G. Song, and P. N. Roy, J. Chem. Phys. **120,** 5916 (2004).
[212] M. Fárník, B. Samelin, and J. P. Toennies, J. Chem. Phys. **110,** 9195 (1999).
[213] A. Scheidemann, B. Schilling, and J. P. Toennies, J. Phys. Chem. **97,** 2128 (1993).
[214] K. W. Jucks and R. E. Miller, J. Chem. Phys. **88,** 2196 (1988).
[215] D. S. Anex, E. R. Davidson, C. Douketis, and G. E. Ewing, J. Phys. Chem. **92,** 2913 (1988).
[216] B. J. Howard, T. R. Dyke, and W. Klemperer, J. Chem. Phys. **81,** 5417 (1984).
[217] M. Quack and M. A. Suhm, J. Chem. Phys. **95,** 28 (1991).
[218] B. Kuhn, T. R. Rizzo, D. Luckhaus, M. Quack, and M. A. Suhm, J. Chem. Phys. **111,** 2565 (1999).
[219] J. Koput, S. Carter, and N. C. Handy, J. Phys. Chem. A **102,** 6325 (1998).
[220] D. Blume, M. Lewerenz, F. Huisken, and M. Kaloudis, J. Chem. Phys. **105,** 8666 (1996).
[221] F. Huisken, E. G. Tarakanova, A. A. Vigasin, and G. V. Yukhnevich, Chem. Phys. Lett. **245,** 319 (1995).
[222] F. Huisken, M. Kaloudis, A. Kulcke, C. Laush, and J. M. Lisy, J. Chem. Phys. **103,** 5366 (1995).
[223] G. E. Douberly and R. E. Miller, J. Phys. Chem. B **107,** 4500 (2003).
[224] D. T. Moore and R. E. Miller, J. Chem. Phys. **118,** 9629 (2003).
[225] D. T. Moore and R. E. Miller, J. Chem. Phys. **119,** 4713 (2003).
[226] D. T. Moore and R. E. Miller, J. Phys. Chem. A **107,** 10805 (2003).
[227] D. T. Moore and R. E. Miller, J. Phys. Chem. A **108,** 1930 (2004).
[228] D. R. Lide, ed., *CRC Handbook of Chemistry and Physics*, vol. 71 (CRC Press, Boca Raton, 1990).
[229] B. R. Strazisar, C. Lin, and H. F. Davis, Science **290,** 958 (2000).
[230] I. W. M. Smith and F. F. Crim, Phys. Chem. Chem. Phys. **4,** 3543 (2002).
[231] M. Bittererova, H. Ostmark, and T. Brinck, Chem. Phys. Lett. **347,** 220 (2001).
[232] M. Bittererova, H. Ostmark, and T. Brinck, J. Chem. Phys. **116,** 9740 (2002).
[233] P. Zhang, K. Morokuma, and A. M. Wodtke, J. Chem. Phys. **122,** 014106 (2005).
[234] F. Cacace, G. de Petris, and A. Troiani, Science **295,** 480 (2002).
[235] N. Hansen and A. M. Wodtke, J. Phys. Chem. A **107,** 10608 (2003).
[236] E. B. Gordon, L. P. Mezhov-Deglin, O. F. Pugachev, and V. V. Khmelenko, Chem. Phys. Lett. **54,** 282 (1978).
[237] E. B. Gordon, V. V. Khmelenko, A. A. Pelmenev, E. A. Popov, and O. F. Pugachev, Chem. Phys. Lett. **155,** 301 (1989).
[238] E. B. Gordon, V. V. Khmelenko, A. A. Pelmenev, E. A. Popov, O. F. Pugachev, and A. F. Shestakov, Chem. Phys. **170,** 411 (1993).
[239] R. E. Boltnev, E. B. Gordon, V. V. Khmelenko, I. N. Krushinskaya, M. V. Martynenko, A. A. Pelmenev, E. A. Popov, and A. F. Shestakov, Chem. Phys. **189,** 367 (1994).
[240] R. Côté, V. Kharchenko, and M. D. Lukin, Phys. Rev. Lett. **89,** 093001 (2002).
[241] E. B. Gordon, private communication with R. E. Miller (2000).
[242] E. B. Gordon, A. A. Pelmenev, O. F. Pugachev, and V. V. Khmelenko, Chem. Phys. **61,** 35 (1981).
[243] R. E. Boltnev *et al*., in *55th International Symposium on Molecular Spectroscopy* (Ohio State University, Columbus, OH, USA, 2000), WI13, p. 183.
[244] E. A. Popov *et al*., in *55th International Symposium on Molecular Spectroscopy* (Ohio State University, Columbus, OH, USA, 2000), WI14, p. 183.
[245] E. B. Gordon, Low. Temp. Phys. **30,** 756 (2004).
[246] R. D. Etters, J. V. Dugan Jr, and R. W. Palmer, J. Chem. Phys. **62,** 313 (1975).
[247] I. F. Silvera and J. T. M. Walraven, Phys. Rev. Lett. **44,** 164 (1980).
[248] E. S. Meyer, Z. Zhao, J. C. Mester, and I. F. Silvera, Phys. Rev. B **50,** 9339 (1994).
[249] E. A. Cornell and C. E. Wieman, Rev. Mod. Phys. **74,** 875 (2002).
[250] W. Ketterle, Rev. Mod. Phys. **74,** 1131 (2002).
[251] M. M. Nieto, M. H. Holzscheiter, and T. J. Phillips, J. Opt. B **5,** S547 (2003).
[252] M. G. Kozlov and A. Derevianko, Phys. Rev. Lett. **97,** 063001 (2006).
[253] S. Y. T. van de Meerakker, P. H. M. Smeets, N. Vanhaecke, R. T. Jongma, and G. Meijer, Phys. Rev. Lett. **94,** 023004 (2005).
[254] A. V. Avdeenkov and J. L. Bohn, Phys. Rev. Lett. **90,** 043006 (2003).
[255] A. V. Avdeenkov and J. L. Bohn, Phys. Rev. A **66,** 052718 (2002).

[256] N. Mudrich, O. Bünermann, F. Stienkemeier, O. Dulieu, and M. Weidemüller, Eur. Phys. J. D **31,** 291 (2004).
[257] F. Stienkemeier, F. Meier, A. Hagele, H. O. Lutz, E. Schreiber, C. P. Schulz, and I. V. Hertel, Phys. Rev. Lett. **83,** 2320 (1999).
[258] C. P. Schulz, P. Claas, and F. Stienkemeier, Phys. Rev. Lett. **8715,** 153401 (2001).
[259] G. Droppelmann, O. Bünermann, C. P. Schulz, and F. Stienkemeier, Phys. Rev. Lett. **93,** 023402 (2004).
[260] G. Scoles, ed., *Atomic and Molecular Beam Methods*, vol. 1 (Oxford University Press, New York, 1988).
[261] W. B. Zeimen, J. A. Kłos, G. C. Groenenboom, and A. van der Avoird, J. Phys. Chem. A **108,** 9319 (2004).
[262] S. Goyal, D. L. Schutt, and G. Scoles, Phys. Rev. Lett. **73,** 2512 (2004)